THE SENSITIVITY OF A GENERAL CIRCULATION MODEL CLIMATE TO THE MOISTURE TRANSPORT FORMULATION*

Philip J. Rasch and David L. Williamson
National Center for Atmospheric Research**
Boulder CO, USA

1. INTRODUCTION

Processes associated with water in the atmosphere are particularly difficult to model accurately. There are very large horizontal and vertical spatial variations in the moisture field, and very strong and small scale sources and sinks of moisture associated with phase change. Yet because it is such a radiatively important constituent both in vapor and cloud forms, and because the heat release associated with phase change can be large, it is critical to model reasonably accurately the processes which affect the distribution of water.

In this paper some aspects of two very different numerical methods (spectral and semi-Lagrangian) used to approximate the transport of water vapor in the NCAR Community Climate Model (CCM1) are examined. We have recently been investigating the use of semi-Lagrangian transport (SLT) methods as an alternative to spectral methods for the advection of moisture in global atmospheric models [*Rasch and Williamson*, 1990a; *Rasch and Williamson*, 1990b; *Williamson and Rasch*, 1989; *Williamson*, 1990]. In *Rasch and Williamson* [1990b] we described the computational differences between these methods and characterized them in terms of a set of desirable computational properties.

This paper documents the way the algorithmic differences are manifested in the climate of the model. The climate of the model changes significantly when the spectral transport scheme is replaced by the semi-Lagrangian scheme. These changes provide information about the sensitivity of model processes to the water vapor distribution, information about the interaction of various processes via feedback mechanisms, and clues to deficiencies in the model associated with the computational methods themselves.

The characteristics of the model used in the simulations are described in section 2. Section 3 outlines our experimental strategy, and provides some cautionary notes about the interpretation of the simulations. Section 4.1 documents the change in climate in terms of the water vapor, temperature, and cloud distribution. The climate changes are then interpreted by examining selected terms in the thermodynamic budget (in section

---

* A longer version of this report has been accepted for publication in the Journal of Geophysical Research to appear in 1991

** The National Center for Atmospheric Research is sponsored by the National Science Foundation

4.2), first for the polar regions and then for the mid-latitudes and tropics. These terms are obviously sensitive to the water vapor distribution, and in section 4.3 the dominant terms in the moisture budget are described. In section 5 we make some remarks about the importance of these results with respect to changes in the parameterization of other processes in atmospheric models and summarize the study.

2. MODEL DESCRIPTION

As in *Rasch and Williamson* [1990b], the spectral (which we also call the control) version of the model is the NCAR CCM version 1 [*Williamson et al.*, 1987; *Hack et al.*, 1989]. The simulations are carried out at T42 resolution, using an approximately 2.8 degree Gaussian grid, with 12 unequally spaced vertical levels. The finite difference representations of the vertical derivatives are only first-order accurate for unequally spaced levels. The model is based on the primitive equations with $\sigma = p/p_s$ as the vertical coordinate; p is pressure and p_s is surface pressure. The sigma values of the 12 levels are 0.991, 0.926, 0.811, 0.664, 0.500, 0.355, 0.245, 0.165, 0.110, 0.060, 0.025, 0.009. The model contains a Manabe-style deep convective adjustment parameterization and a large-scale stable condensation parameterization [*Manabe, Smagorinsky and Strickler*, 1965]. No diurnal cycle is used, and an instantaneous energy balance is assumed at the surface. Simple bulk aerodynamic parameterizations of surface exchange, and subgrid-scale vertical diffusion are included. The model contains a gravity wave drag parameterization following *McFarlane* [1987]. Radiatively active clouds are formed that depend upon the characteristics of the convective processes and large-scale condensation to define the location, depth and some of the optical properties of the cloud. A description of the cloud scheme and associated radiative properties may be found in *Kiehl and Ramanathan* [1990]. The cloud emissivity is proportional to the amount of water condensed at that level at that timestep. The cloud albedo is a specified function of level. All evolution equations use the spectral transform formalism for the horizontal terms and conserving finite differences for the vertical.

Spectral atmospheric model simulations such as those produced by the control model can be corrupted by negative values of water vapor that are generally "fixed" in some fashion [*Rasch and Williamson*, 1990b]. They are also subject to "spectral rain" [*Williamson*, 1990] caused by overshoots introduced by the spectral representation, which cannot be monitored or fixed, and they are "non-local" in the sense that the solution at a given location can be affected by processes operating far away and downwind from that point. Shape preserving SLT methods do not suffer from these particular drawbacks. They do not generate overshoots or undershoots (new maxima or minima) due to numerical deficiencies. Thus the numerical scheme cannot introduce negative values, or supersaturation.

They transport information downwind only, and are sensitive to the local characteristics of the wind and moisture fields only.

Because of these desirable transport properties, and also because of their unconditional stability, SLT methods have been receiving increasing attention in atmospheric modeling. For the modified version of the model the spectral/finite difference transport of water vapor specific humidity, q, is replaced with a three-dimensional semi-Lagrangian transport algorithm. Earlier we have examined the behavior of both the "standard" semi-Lagrangian transport, which uses Lagrange polynomial interpolation [e.g. *Ritchie* [1985]] and "shape-preserving" semi-Lagrangian transport, which can use a variety of shape preserving interpolation forms [details may be found in *Rasch and Williamson* [1990b], *Williamson and Rasch* [1989] and *Williamson* [1990]].

Based on our earlier studies the configuration we have chosen for the interpolant is Hermite cubic with a cubic derivative estimate modified to be monotonic (Hermite/cubic/SCM0 in the notation of the earlier papers). When the field to be represented is smooth, and away from extrema, this interpolant results in a formally fourth-order accurate scheme. Thus, the scheme is formally of a lower order of accuracy in the horizontal when compared to spectral method, and of a higher accuracy in the vertical when compared to the vertical finite differences. Where the solution is discontinuous (and the formal concept of accuracy is meaningless), and in the vicinity of extrema, the accuracy of the shape preserving methods is deliberately reduced in order to enforce the physical requirement that the advection introduces no new extrema, i.e., it eliminates over- and undershooting.

SLT schemes are not inherently conservative. We enforce conservation explicitly in the SLT simulations discussed in this paper at every time step through a variational adjustment of the specific humidities which weights the amplitude of the adjustment in proportion to the advection tendencies and the field itself [*Rasch and Williamson*, 1990b; *Sasaki*, 1976; *Isaacson*, 1977; *Takacs*, 1988]. This adjustment is typically small, with the largest relative changes no larger than 7% of those of the advective tendencies at the same gridpoint. Enforcement of conservation in an *a posteriori* fashion should be considered a stopgap measure and used cautiously. *Takacs* [1988] has shown that *a posteriori* conservation of mass and energy did not improve the accuracy of solutions using either first- or fourth-order accurate schemes. *Brackbill and Margolin* [1977] have shown some schemes that impose energy conservation exhibit an instability that normally saturates at a finite amplitude. Both papers suggest that constraint restoration used with accurate schemes does little to the local details of a simulation. Our conservation fixer differs in many details from these studies (e.g., it is scale selective), but we believe this conclusion carries over. We have

repeated the tests defined in *Williamson and Rasch* [1989] with the conservation fixer in place and were unable to see differences in the contoured solution, and as we show below, we are unable to find evidence of influence of the conservation fixer on the model climate in the CCM. The variational adjustment does not tend to improve or degrade the accuracy of the unadjusted scheme, it merely enforces the constraint.

As mentioned earlier, the shape preserving SLT prevents any "overshoot" or "undershoot" in the solution due to the numerical advection algorithms, and thus prevents both negative specific humidities and "spectral" rain. Standard non-shape preserving SLT schemes do not satisfy this property and require "fixers" to maintain positivity like the spectral methods and also require a conservation adjustment like the shape preserving SLT method. We have shown in *Rasch and Williamson* [1990b] that the positivity "fixers" can be an important component of the water vapor budget in the spectral transport algorithm in some regions of the model atmosphere. The interaction of these computational processes with the physical parameterizations will become more apparent in the following analysis.

The desirable characteristics gained by using the SLT algorithm are not without cost when compared to a traditional spectral or finite difference algorithm with the same time step. The codes used for the experiments reported here are experimental and not optimally designed. More effort has been devoted toward developing efficient code for the next model version, CCM2. For a prototype version of CCM2, which is still not optimal, the trajectory calculation and semi-Lagrangian transport of water vapor requires about 16 percent of the model run time. Each additional tracer requires an additional 3 percent of this baseline run time.

3. EXPERIMENTAL DESIGN

All figures in this paper display data following a time averaging of 60 days of the simulation, sampled once daily. The averaging period is centered on January 15th, from the second winter of the simulation with the semi-Lagrangian transport of water vapor (referred to as SLT), and the sixth winter of the simulation with spectral transport (referred to as spectral or control). In the troposphere the SLT simulation has approached its climatological state because it started from the spectral simulation and adjusts to the new climate during the first year of simulation. The lower stratosphere responds more slowly, with small changes in the moisture for the first two years. Because the model is configured with reasonable resolution only in the troposphere we will not emphasize the behavior of the lower stratospheric simulation.

Although we have not performed formal statistical tests for changes in the state variables, we do indicate where those changes in state variables are large with respect to the

variability of the spectral model. The standard deviation of the zonal time average for the six winters of the spectral control was calculated to provide a measure of the interannual variability of fields which enter into the comparison. The differences for the state variables between the SLT and the spectral simulations have been compared to this measure of natural variability. Areas in which the difference is less than three standard deviations are stippled. The variability of the SLT model might be very different from that of the spectral, especially in the polar regions where the schemes have very different characteristics. Our SLT simulation is too short to provide any information about its variability.

4. RESULTS

4.1 Temperature, Moisture and Clouds

We begin by focusing on zonal averages of specific humidity, temperature and cloud fraction in Figs. 1 through 3. The top panel of each displays the time-averaged, zonal average of the field from the SLT simulation. The middle panel displays the corresponding field from the spectral simulation. Differences (SLT-spectral) are shown in the bottom. Regions where the differences are less than three standard deviations are stippled. The actual model levels are indicated by the inner ticks on the left side of each panel. In this section statements such as *drier* or *warmer* will refer to the SLT simulation relative to the spectral unless otherwise stated.

Changing the transport scheme changes the average moisture field significantly (Fig. 1. Note that the contour intervals for the fields themselves are nonuniformly spaced at 1×10^n, and 3×10^n g/kg, approximately uniform after a logarithmic transformation of q, and for the difference field are uniform and equal to 0.1 gm Kg^{-1}.) The SLT simulation is generally moister in the lower tropical and subtropical troposphere ($\approx$ 800 mb) by as much as 0.7 gm Kg^{-1} (25%), and dryer by as much as 0.9 gm Kg^{-1} (30%) above ($\approx$ 600 mb). There is also a significant (but relatively smaller) reduction in specific humidity in the SLT in the extra-tropics extending to 60 or 70 degrees latitude in both hemispheres. There are notable changes at the South Pole, with increases in specific humidity at lower levels (1000 to 700 mb) and a decrease above 300 mb. These changes at the South Pole seem small when compared to other regions of the troposphere but in fact are very large relative to the local ambient moisture values. There is a significant increase in moisture in the SLT simulation in the surface layer of the northern polar regions. Although less than three standard deviations, much of the difference in the stippled areas of the polar regions exceeds two standard deviations with respect to the interannual variability of the spectral simulations.

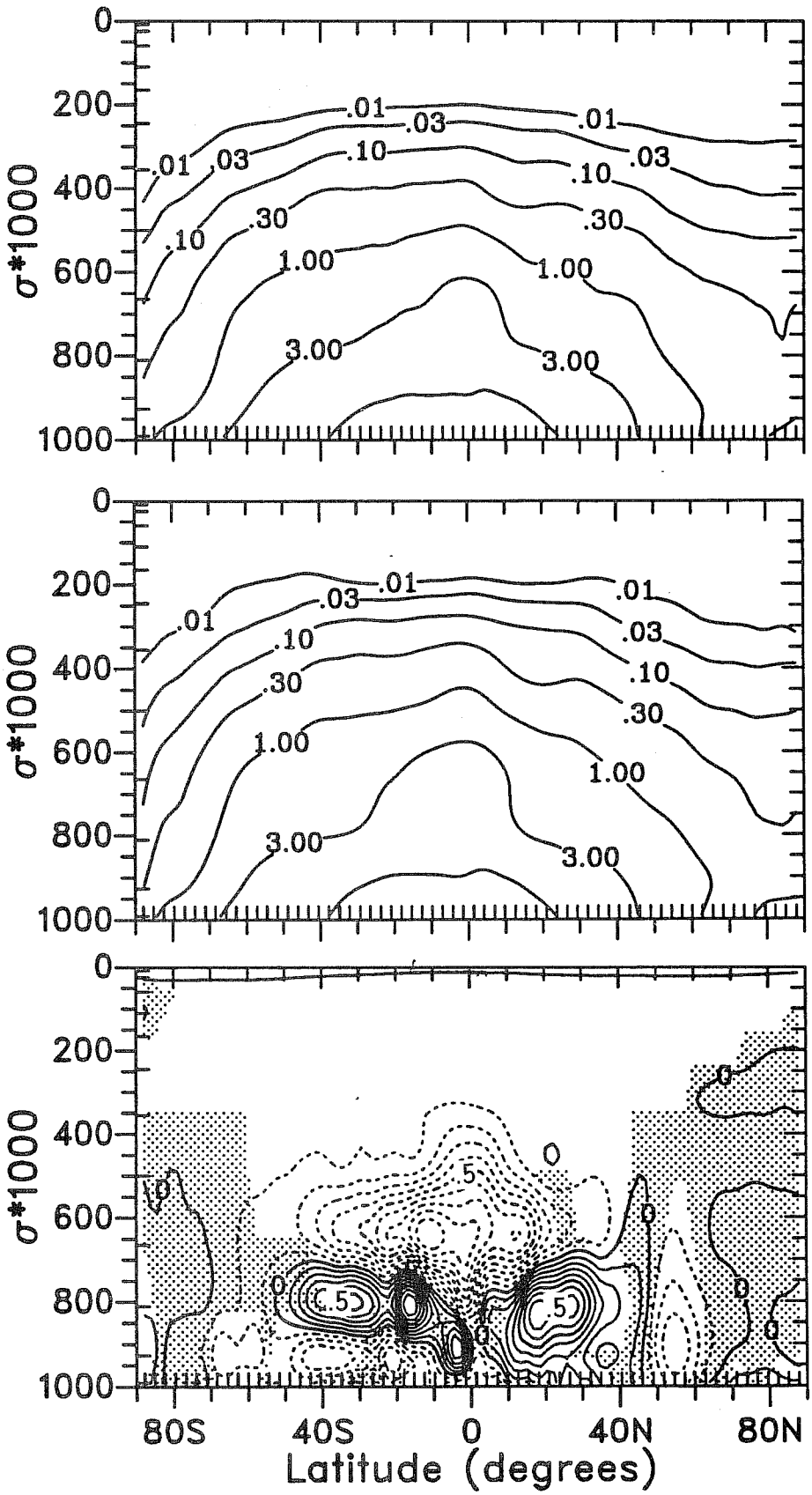

Fig. 1 *Top Panel:* Zonal average of the time-averaged specific humidity for the SLT simulation. Contours values are 3 x 10^n and 1 x 10^n gm Kg^{-1}. *Center Panel:* same for spectral simulation. *Bottom Panel:* differences (SLT-spectral) of the specific humidity with a contour interval of 0.1 gm Kg^{-1}. Areas where difference is less than 3 standard deviations of the averages of the spectral simulation are stippled. See text for details.

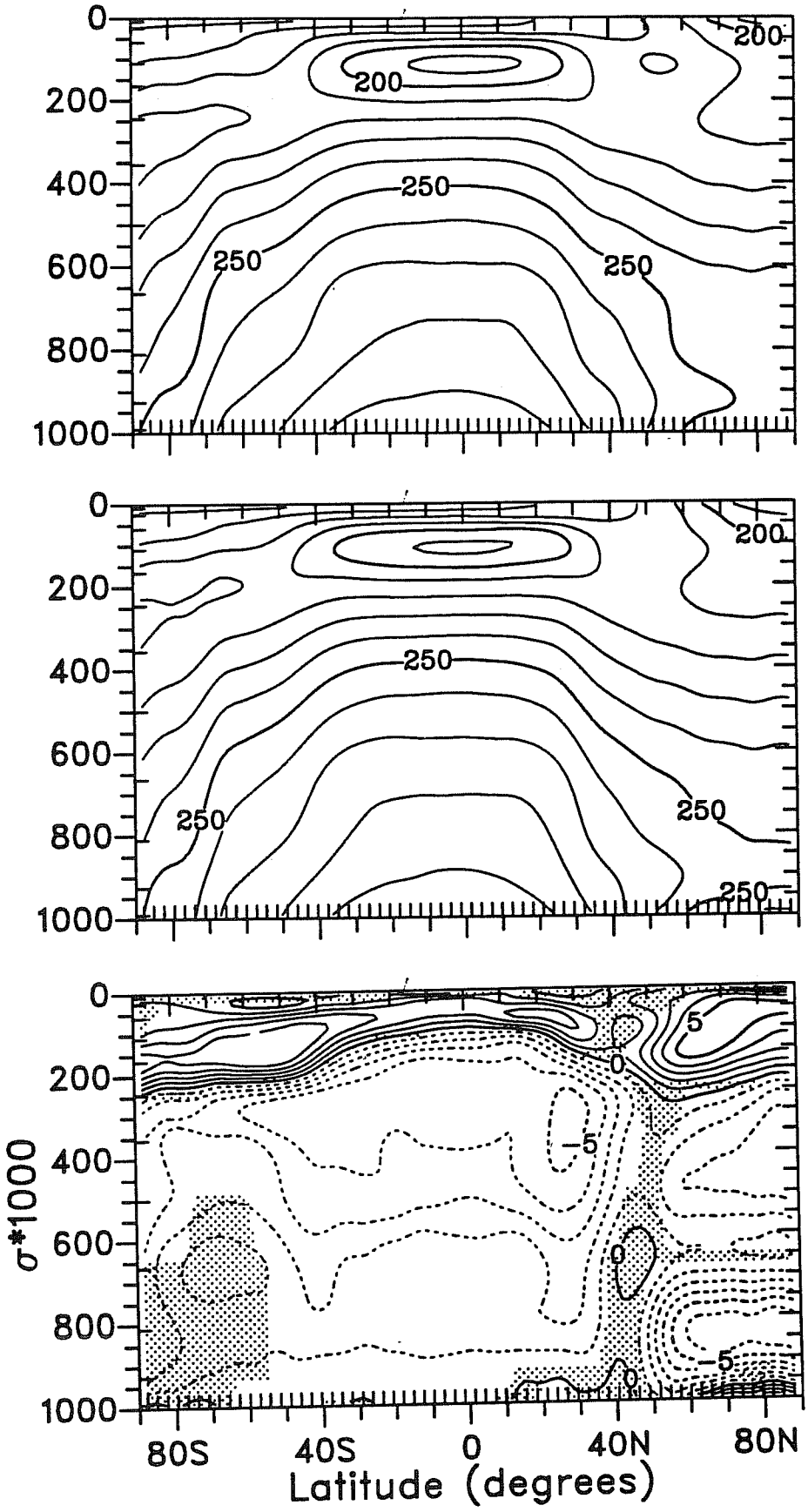

Fig. 2 As in Fig. 1, except for temperature. Contour interval is 10.0 K for fields, 1.0 K for differences.

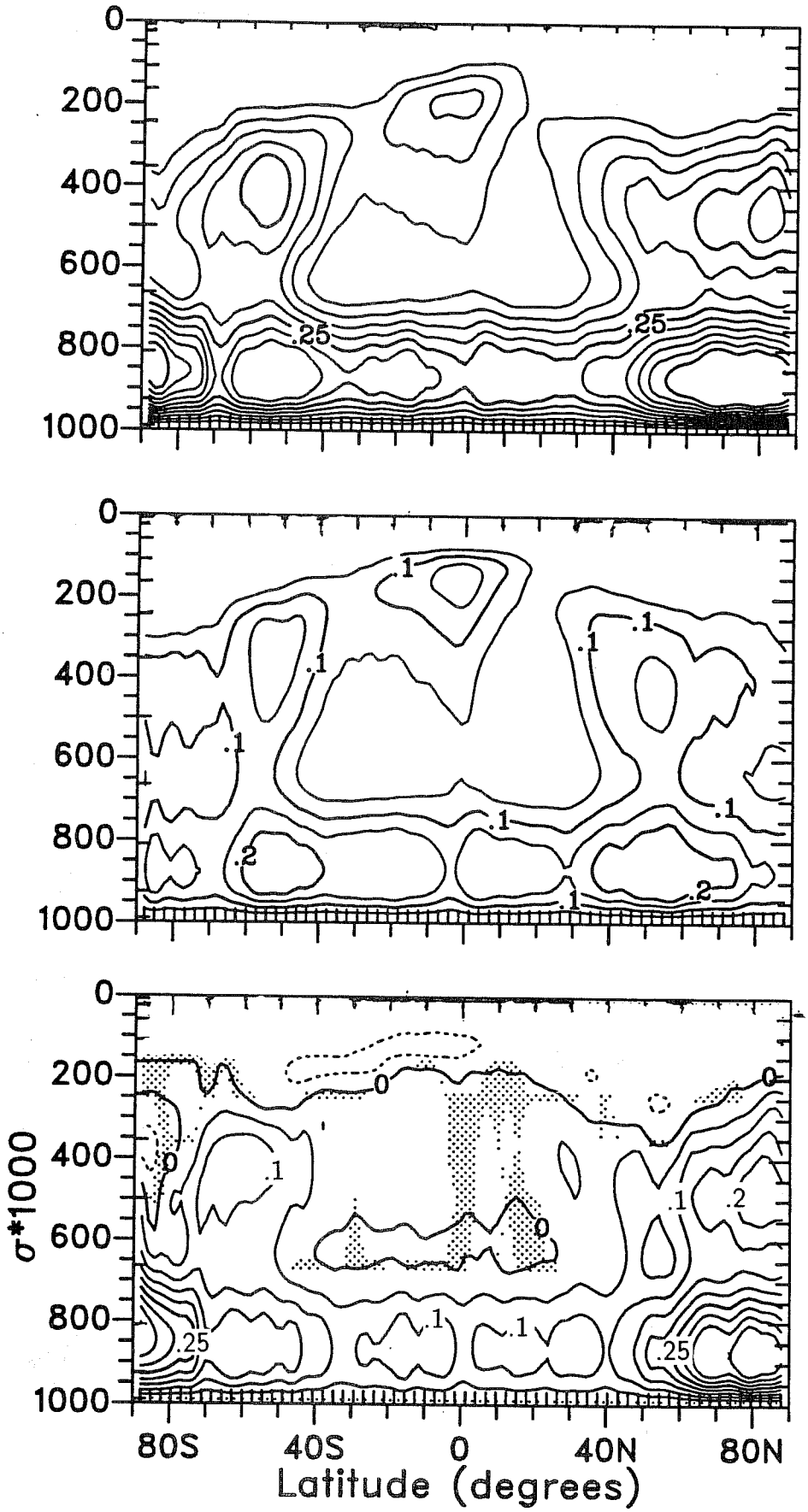

Fig. 3 As in Fig. 1, except for cloud fraction. Contour interval is 0.05.

The dry stratosphere in both simulations is a characteristic of versions of this model when very few (3) levels are present in the stratosphere. Increasing the vertical resolution in the stratosphere results in a substantial increase in the moisture there (not shown).

The total atmospheric moisture (global average precipitable water, not shown) is generally too small in both simulations (20 kg/m^2 in the spectral, 19.5kg/m^2 in the SLT) when compared to observations [$\sim$24kg/m^2, c.f. *Peixoto and Oort* [1983], *Trenberth, Christy and Olson* [1987]]. The SLT simulation is slightly (3%) drier than the spectral, but both are 20% drier than suggested by the observations. Both simulations are too dry in the polar regions when compared to observations. The change in the moisture distribution and the global average precipitable water is the result of a number of complex feedbacks, some of which we hope emerge in the following discussion.

Fig. 2 displays the zonal average temperature. The cooler troposphere and warmer stratosphere in the SLT simulation are remarkably similar but of opposite sign to the changes seen by *Ramanathan et al.* [1983] when they varied the physical assumptions concerning cloud location and optical properties. Ramanathan et al. increased the emissivity of the high stratus clouds in their experiments. As will be seen shortly, the effective high-level stratus clouds are decreased in the SLT simulation, which is consistent with the observed opposite response.

The tropopause temperature has changed only slightly, with most differences occurring above or below it. There is a general increase in instability in the troposphere of the SLT simulations in the tropics and mid-latitudes because differences in the surface layer temperature are small but the lapse rate to 300 mb is larger. The surface layer temperature over much of the globe is tied closely to the fixed sea surface temperatures of the model. The largest differences in the troposphere occur in the polar night region. The lower tropospheric temperatures are colder ($\approx 6K$), the surface layer temperatures are warmer (by $\approx 3K$), and there is an asymmetry between the winter and summer poles. In the summer polar regions the difference is less than half as large (2 K) with a much smaller vertical gradient.

Clouds, which strongly influence, and are influenced by, the temperature and moisture profiles show dramatic differences (Fig. 3, recall that in this model clouds occur only in the presence of grid cell saturation and condensation or moist convective instability). The SLT simulation has a much larger cloud fraction. The largest increases are located in the lower troposphere but there are also very large *relative* changes in the middle and high clouds in the extratropics. There is a reduction in clouds in the south polar region near 300 millibars, and in the tropics between one and two hundred millibars.

The main difference in the effective cloud (not shown) as seen by the infrared radiation is confined to the region below 600 mb where the cloud emissivities are one, and the difference matches the difference in cloud fraction. The stable cloud emissivities depend on the amount of condensed water per times step q_c in the layer

$$\epsilon = \begin{cases} \left(1 - e^{-0.1 q_c}\right) / \left(1 - e^{-2.5}\right) & q_c \leq 25 \text{ gm/m}^2 \\ 1.0 & q_c > 25 \text{ gm/m}^2. \end{cases}$$

Above 600 mb, the positive/negative pattern of the effective cloud difference matches that of the cloud fraction difference but the magnitude of the effective cloud difference is on the order of 2.5%. The cloud fraction difference in the region of 300 to 600 mb of 10% in the Southern Hemisphere and 20% in the Northern Hemisphere are not seen in the effective clouds. As will be seen later when the moisture budget is considered, more stable condensation occurs in these regions in the spectral simulation than in the SLT.

The global average total fractional cloudiness, using a random overlap assumption, has increased from 40% in the spectral to 50% in the SLT simulation. Large increases in cloudiness are evident in the southern mid-latitudes, a clear improvement. Increases over the Northern Hemisphere storm tracks, and off the coast of the Baja peninsula are also apparent. The clouds associated with deep convective events over the Amazon and South Africa have also increased.

The improvement in the cloud distribution can be seen more readily using the quantitative measures in Fig. 4, which compare the long and short wave cloud radiative forcing [LWCF and SWCF respectively, *Ramanathan* [1987], *Slingo and Slingo* [1988], *Kiehl and Ramanathan* [1990]] for the two simulations with Earth Radiation Budget Experiment (ERBE) data for January of 1986. The fields represent the difference between estimates of the top of atmosphere clear sky and total radiative fluxes, and as such are a column integrated measure of the effect of clouds on the surface/atmosphere system. A reduction in the longwave emission by clouds appears as a positive longwave cloud forcing. A reduction of the solar radiation by clouds appears as a negative shortwave cloud forcing. The LWCF is weighted most strongly by the radiative effect of optically thick, deep clouds with cold, high tops. The SWCF, sensitive to low clouds associated with cyclogenesis and oceanic stratus decks, is felt most strongly at the surface. The ERBE data are reported by *Kiehl and Ramanathan* [1990] to be accurate to $\pm$ 10 W/M^2 on the 2.5° grid, with less accuracy poleward of 60°. Thus, the positive values of SWCF in the ERBE data seen near the South Pole should be disregarded. The largest difference in cloud radiative forcing occurs in the southern mid-latitudes where the shortwave cloud forcing has increased from about 80 Watts/M^2 in the spectral simulation to about 120 Watts/M^2, substantially nearer the observed 160 Watts/M^2. There is a corresponding change in the longwave part of the spectrum at the same latitudes. The weak cloud forcing compared to the observed in the northern mid-latitudes and equatorial regions is suggestive of insufficient high cloud amount or underestimated emissivities in those regions.

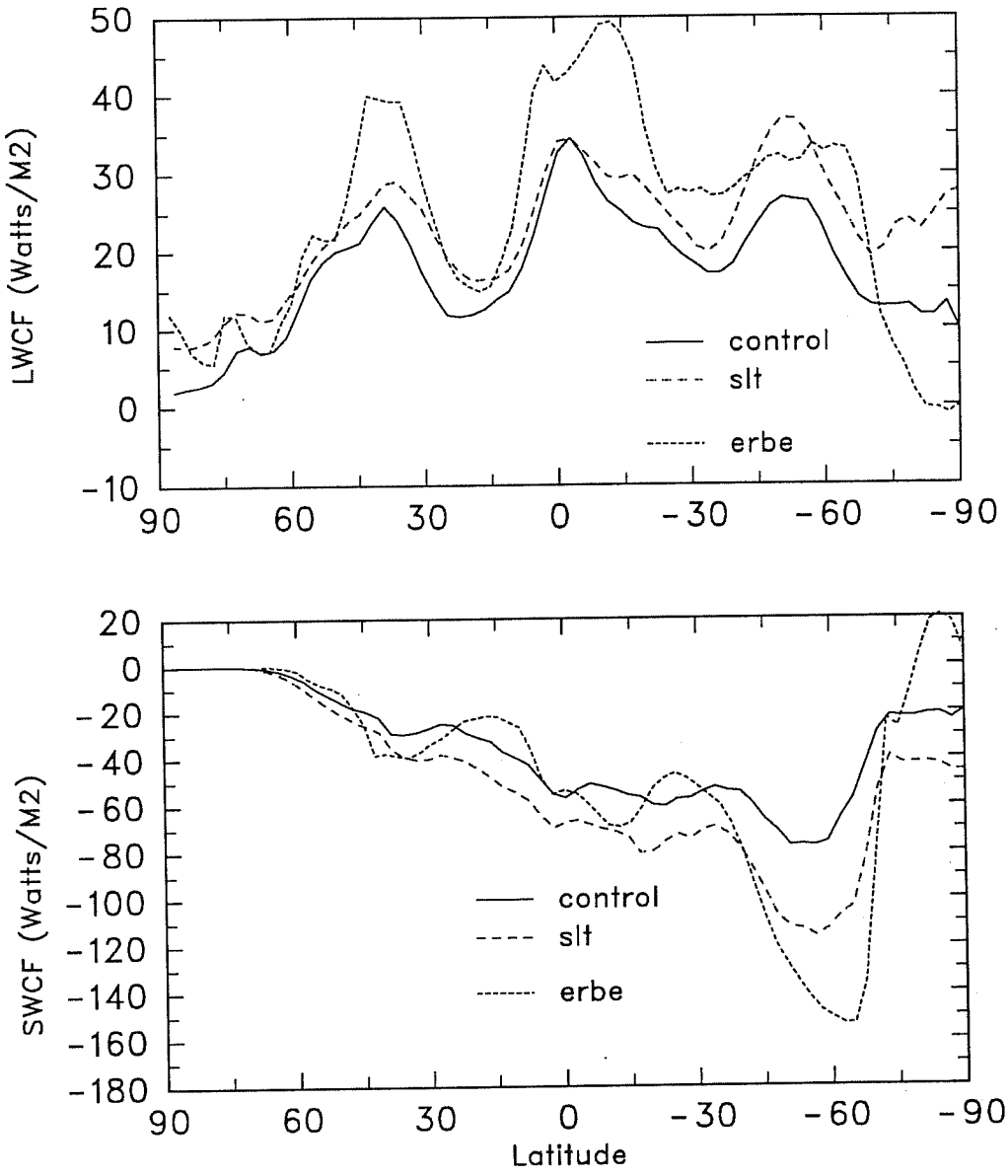

Fig. 4 Zonal averages of the top of atmosphere cloud radiative forcing for the spectral and SLT version of the model, compared with the January 1986 average of the observed cloud forcing from ERBE. Units are Watts/M^2. *Top Panel:* longwave cloud forcing (LWCF). *Bottom Panel:* shortwave cloud forcing (SWCF).

4.2 Thermodynamic Budget

It is interesting to contrast the change in the simulation poleward of 50 degrees in the summer and winter hemispheres, where the relative change in low clouds is similar, but the temperature response is different. The relative humidity has increased and the temperature has decreased at both poles, but the temperature decrease is much larger at the winter pole. Some insight may be gained into the processes responsible for this different response by examining the various terms of the thermodynamic equation. These terms are presented in Figs. 5–8. The longwave radiative cooling appears in Fig. 5 (negative for cooling, positive for heating), the temperature tendency associated with diabatic moist processes is shown in Fig. 6. The sum of the vertical and horizontal diffusion and the surface fluxes of heat appears in Fig. 7, and the forcing associated with the dynamical terms (vertical and horizontal temperature advection, and the energy conversion term) appears in Fig. 8. The solar heating in the atmosphere which is not shown, is very similar in the two simulations. This similarity is presumably due to assumptions in the CCM shortwave formulation concerning the distribution of heating in the presence of overlapped clouds, where the flux divergence between the top of the highest cloud and the surface is shared uniformly between model layers.

The differences in the longwave radiative cooling between the simulations are large and coherent (Fig. 5). (In this and the following figures, we dispense with stippling regions where the differences exceed three standard deviations.) The cooling is much stronger in the SLT simulation above the low clouds at all latitudes, and weaker below this level. Thus, the longwave radiation acts to increase the instability of the lower portion of the atmospheric column in the SLT simulation relative to the spectral control, and a response is seen in the moist diabatic processes (Fig. 6), which are much more active in the lower troposphere in the SLT simulation. The sensible heat flux from the surface, which is included with the diffusion term (Fig. 7), is larger in the SLT simulation in the extra-tropics and polar regions, and slightly smaller in the tropics. Although the first two processes examined seemed to be behaving the same way at all latitudes the surface fluxes indicate that the actual balance of terms is very different in various regions. Therefore, we consider each region separately. We first examine the balance at the summer (south) pole. This is followed by a description of the balance at the winter (north) pole and then by a discussion of thermodynamics in the equatorial region.

South Polar Region: The largest difference in longwave cooling occurs at the summer (south) pole. At $\sigma \approx 0.811$ the difference is about 2.6 K d^{-1}, with a reduction in the cooling below of about 1.2 K d^{-1}. The dipole structure in the moist diabatic forcing at the South Pole in the SLT simulation is associated with the moist convective adjustment process

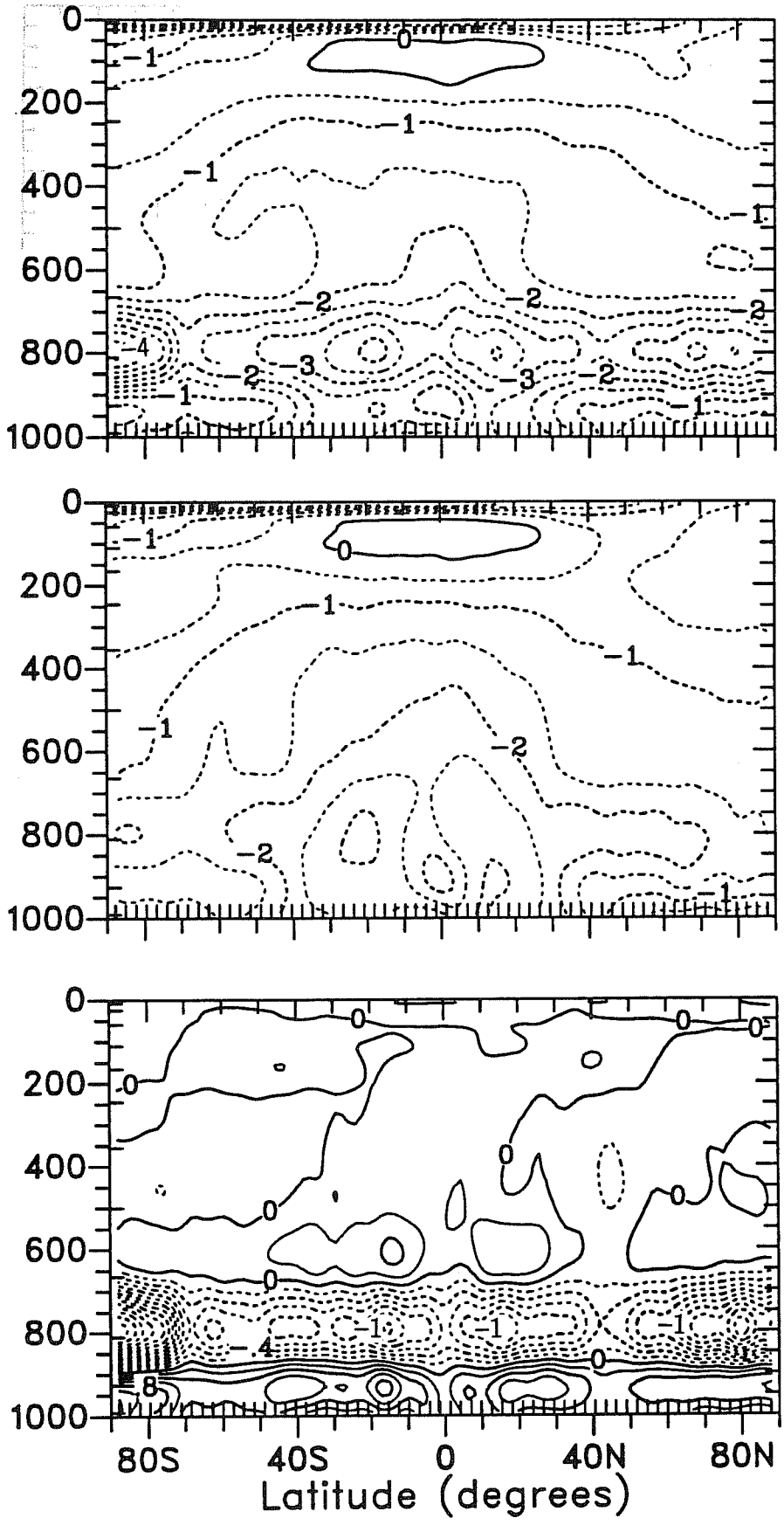

Fig. 5 Time averaged zonal average of the longwave radiative forcing. *Top Panel:* SLT (contour interval, 0.5 K d^{-1}). *Center Panel:* Spectral (contour interval, 0.5 K d^{-1}). *Bottom Panel:* Differences, SLT-spectral (contour interval, 0.2 K d^{-1}).

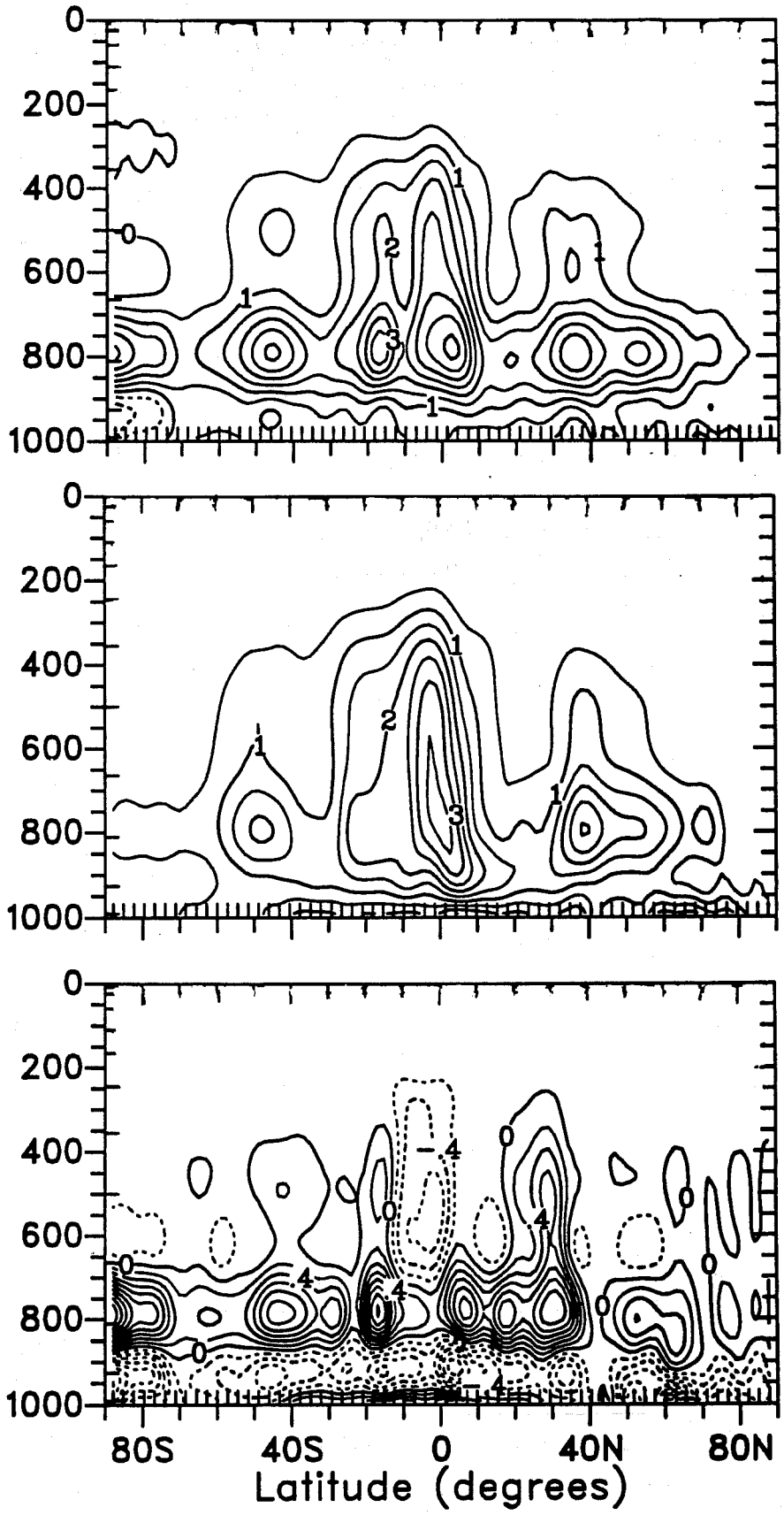

Fig. 6 Time-averaged zonal average of the heating associated with the convective and stable condensation parametrizations. *Top Panel:* SLT (contour interval, 0.5 K d^{-1}). ***Center Panel:*** Spectral (contour interval, 0.5 K d^{-1}). *Bottom Panel:* Differences (contour interval, 0.2 K d^{-1}).

which acts to move heat out of the the surface layer (1.0 K d^{-1} cooling) and into the 0.811σ level (2.5 K d^{-1} heating). The spectral simulation has a similar structure but is much weaker. This heating is *not* due to latent heat release (which is negligible as will be apparent later when the moisture budget is considered), but rather to the overturning associated with the moist adjustment process. Neither model includes dry convective adjustment in the troposphere. Thus, in the SLT simulation the moist convective adjustment is acting primarily as a dry overturning due to destabilization by cloud top cooling. The cooling by moist diabatic processes near the surface in the SLT simulation should be contrasted with a heating in the spectral simulation. A large part of this heating in the surface layer in the spectral run (0.5 K d^{-1}) is associated with condensation of moisture. The source for this moisture in the spectral simulation will later be shown to be the computational filler included in the spectral model to remove negative moisture values.

The vertical gradient of the moist diabatic heating below 500 mb has the same sign for the two simulations (i.e., to increase the stability), but the SLT heating is much stronger, and acts to balance the stronger radiative cooling. There is also an increase in the dynamical heat transport in the SLT simulation at the South Pole, except at the surface layer, where the heating is reduced (Fig. 8). At the 0.811σ level, the dynamical heating has increased by $\approx$ 0.5 K d^{-1} at the summer pole which also helps to compensate the longwave cooling.

The decrease in stability in the SLT simulation is reflected in a slight increase in heat transported via vertical diffusion. The changes in diffusion (and surface flux) tendencies are smaller and less coherent than the previously mentioned processes, although the reader is cautioned that the contour interval is twice that of the previous figures to allow later discussion of the tropical and Northern Hemisphere surface layer tendencies.

Overall the major components (radiative cooling, convective overturning, and dynamic warming) are much more vigorous at the summer pole at $\approx$ 800 mb in the SLT simulation with the diffusion and surface heat flux and the solar heating remaining essentially unchanged.

North Polar Region: The radiative cooling (Fig. 5) again is stronger in the SLT simulation but the differences are somewhat smaller than those seen at the South Pole. The cooling in the SLT simulation has increased at 0.811σ by about 1.4 K d^{-1} and decreased by 0.6 K d^{-1} near the surface. Thus, the increase in forcing toward an unstable column in the SLT simulation is somewhat less at the North Pole than that at the South Pole. The moist diabatic processes (Fig. 6) which were relatively inactive in the spectral simulation at the South Pole are somewhat more active at the North Pole. These terms are small in the SLT simulation. In the spectral simulation the stable condensation is partially balancing

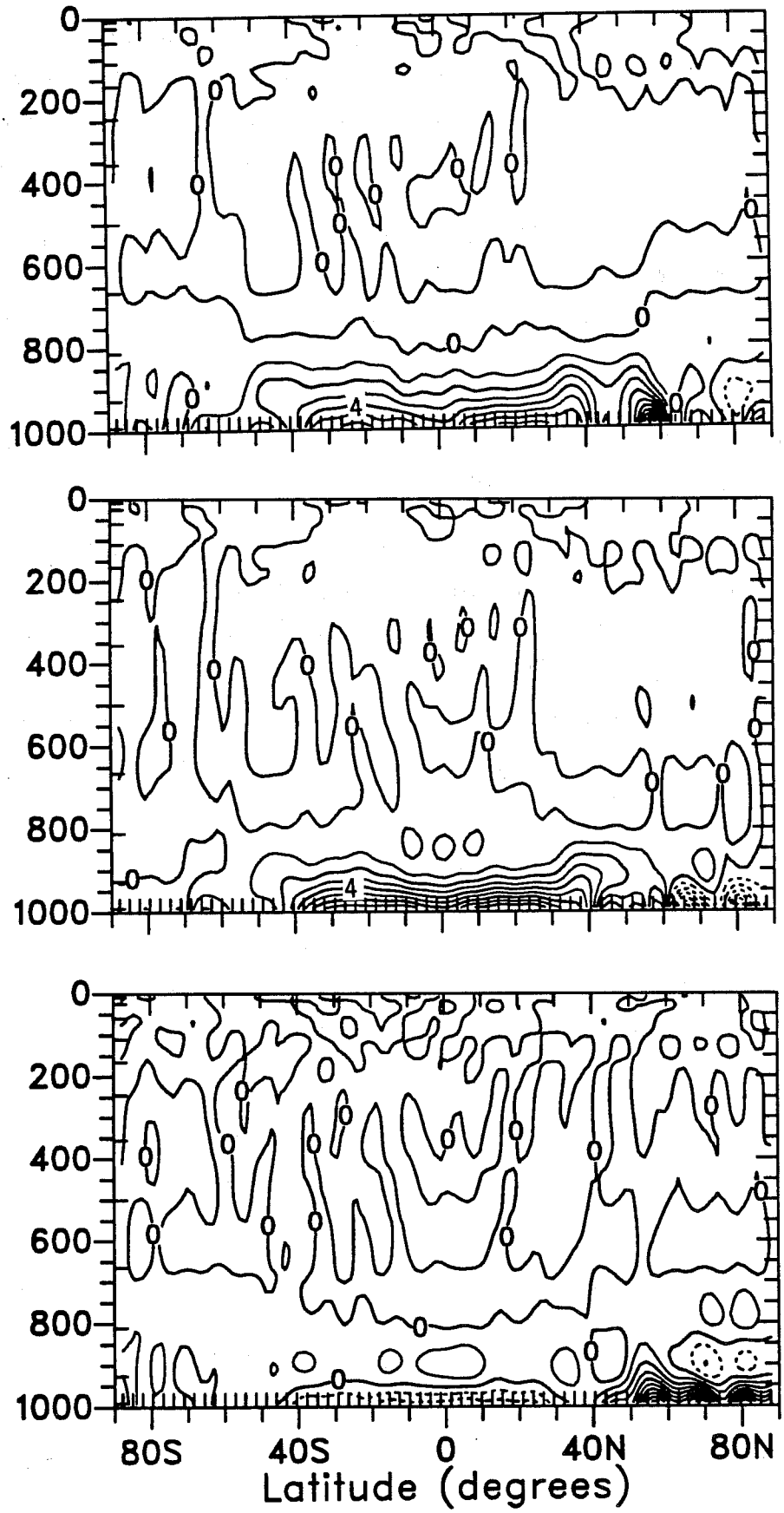

Fig. 7 Time-averaged zonal average of the heating associated with the vertical diffusion and surface sensible heat flux. *Top Panel:* SLT (contour interval, 1.0 K d^{-1}). *Center Panel:* Spectral (contour interval, 1.0 K d^{-1}). *Bottom Panel:* Differences (contour interval, 0.4 K d^{-1}).

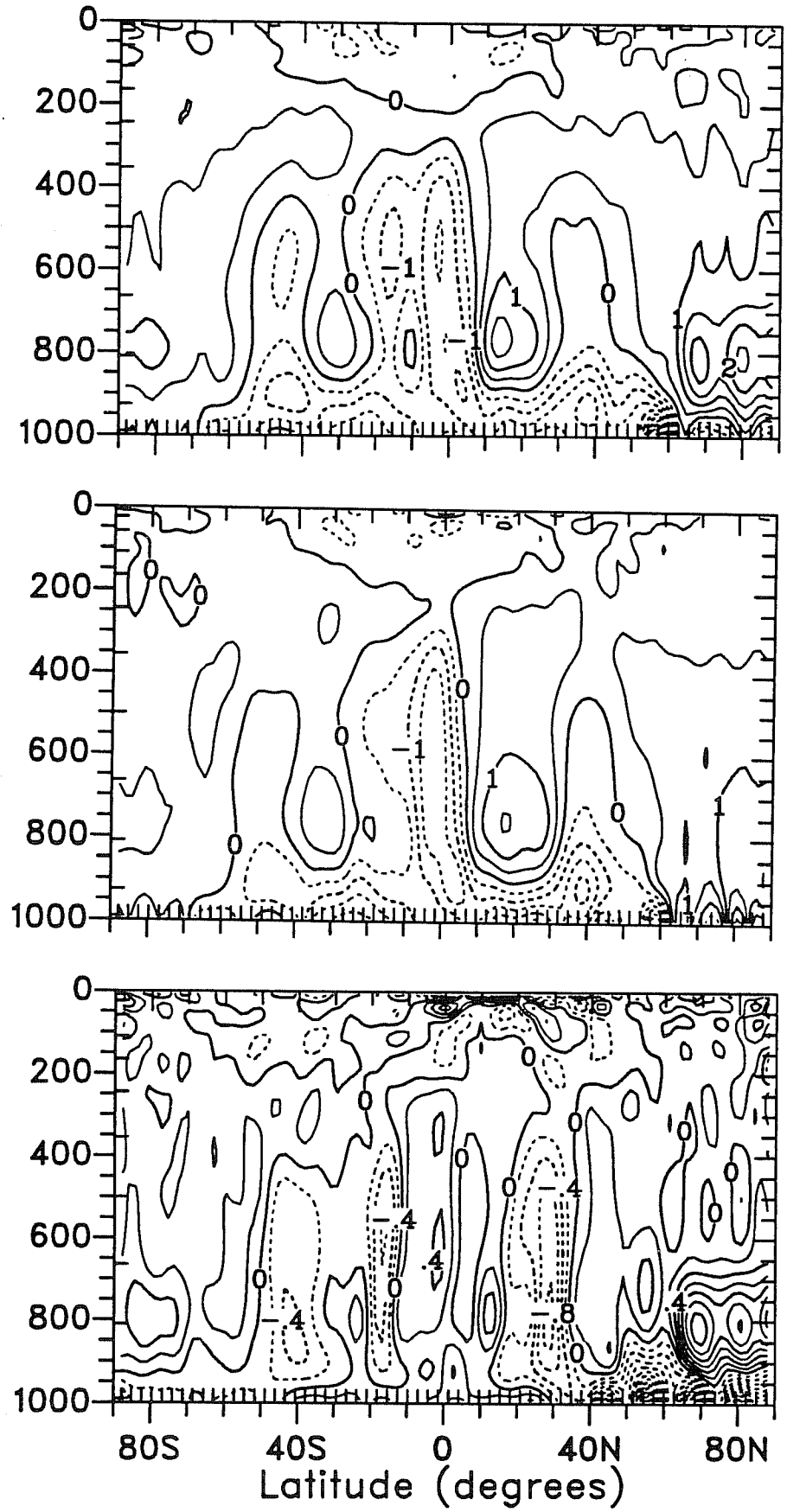

Fig. 8 Time-averaged zonal average of the dynamical heating (advection plus energy conversion term. *Top Panel:* SLT (contour interval, 0.5 K d^{-1}). *Center Panel:* Spectral (contour interval, 0.5 K d^{-1}). *Bottom Panel:* Differences (contour interval, 0.2 K d^{-1}).

the radiative cooling; the difference in moist processes (due to stable condensation in the spectral simulation) is partially balancing the difference in radiative cooling. Near the winter pole dynamical warming (Fig. 8) plays a larger role than moist diabatic heating in balancing the radiative cooling especially in the SLT simulation. The dynamical warming is from both the vertical and horizontal components. The dynamical heating at 0.811σ is much stronger, changing from about 1 K d^{-1} in the spectral, to $2 - 2.5$ K d^{-1} in the SLT simulation. Near the surface in the control run the dynamical terms act to warm the atmosphere (although a fair degree of noise appears in the latitudinal structure), while in the SLT simulation they cool it. This difference is due primarily to a change in the vertical processes at the first model level. Poleward of 60° N the diffusion and surface sensible heat flux terms (Fig. 7) play an important role in the spectral simulation, but are a small component of the balance of the SLT simulation. In the spectral run these terms provide the cooling at the surface to partially balance the moist diabatic heating there.

Overall, at the winter pole at ≈800 mb in the SLT simulation an approximate balance exists between radiative cooling (–3.5 K d^{-1}) and dynamical warming (2.5 K d^{-1}) with vertical diffusion and diabatic moist processes making up the difference. In the spectral simulation the radiative cooling is less (1.5 K d^{-1}) again balanced primarily by dynamical warming. At the surface dynamical cooling occurs in the SLT and warming in the control simulation. The stronger moist diabatic heating at the surface is balanced by stronger cooling by the vertical diffusion in the spectral simulation. These terms are relatively weak at that level in the SLT simulation.

Tropics and Mid-latitude Regions: The longwave cooling at 0.811σ (Fig. 5) is also larger in the SLT simulation away from the poles, and there is notably less radiative cooling below this level and slightly less above, consistent with the changes in the clouds. The result of this difference in longwave radiative cooling is to increase the convective instability in the SLT simulation in the lower troposphere and decreased it above, and one sees a corresponding compensation in the the moist diabatic processes (Fig. 6). The moist processes are more intense but do not penetrate as deeply. The dynamical warming and cooling (Fig. 8) are perhaps slightly more intense in the spectral simulation in the tropics (showing a signal reminiscent of the Hadley cell) with the opposite effect in the mid-latitudes, particularly near the surface between 30 and 70°N. (This difference is dominated by differences in the vertical components.) A corresponding signal near the surface in the tropics and mid-latitudes occurs in the diffusion and surface sensible heat flux (Fig. 7), which is acting to move heat out of the surface and into the layers above with less strength in the SLT simulation but more depth.

4.3 Moisture budget

Although the simulations represent a delicate balance between processes, many of the changes in the thermodynamic budget may be interpreted as a response to changes in the longwave radiative cooling which in turn is responding to changes in the cloud field. The cloud field depends critically on the moisture predicted by the model. (Recall that clouds are formed wherever condensation occurs.) Thus some feel for the cause of the change in clouds can be obtained by examining the moisture budget as expressed by the time-averaged moisture evolution equation.

$$\partial\overline{q}/\partial t = \overline{A_h} + \overline{A_v} + \overline{D_h} + \overline{D_v} + \overline{C_s} + \overline{C_c} + \overline{F} \approx 0 \qquad (1)$$

The terms represent, from left to right, the time-averaged tendency of specific humidity, horizontal advection, vertical advection, horizontal diffusion, vertical diffusion, stable condensation, deep convection and the fixer associated with positivity in the spectral or conservation in the SLT. The bar indicates the time averaging operator.

Because of the large spatial variation in the specific humidity this equation emphasizes the properties of the moisture forecast in the lower troposphere equatorward of 60 degrees latitude. Later we will consider the terms in a normalized forecast equation which emphasizes regions where the various processes affect the moisture field rapidly.

Figures 9–13 present time-averaged zonal averages of the various terms from the SLT simulation in the top panel, the spectral simulation in the middle panel and their difference SLT-spectral in the lowest panel. Fig. 9 shows the vertical advection. Except for a small equatorial region the SLT term moistens relative to the spectral/finite difference term (a positive difference indicates the term moistens in the SLT simulation relative to the spectral). The upward branch of the Hadley cell is stronger in the SLT while the drying in the downward branches is slightly weaker and not as deep. This difference is directly attributable to the different vertical advection approximations used in the two simulations. If the vertical finite difference advection scheme of the spectral model is applied to the fields simulated by the SLT model in a diagnostic manner, the resulting vertical advection looks very similar to that of the spectral simulation rather than to that of the SLT simulation.

Although the horizontal advection (Fig. 10) serves to dry the lower troposphere as it moves moisture into the upward branch of the Hadley cell, the SLT version does so with less vigor in the lower two levels relative to the spectral simulation. In contrast to the vertical advection this difference in the horizontal advection is attributable to the different atmospheric states in the two simulations rather than being due to a primary difference between the two numerical schemes. The spectral advection applied diagnostically to the

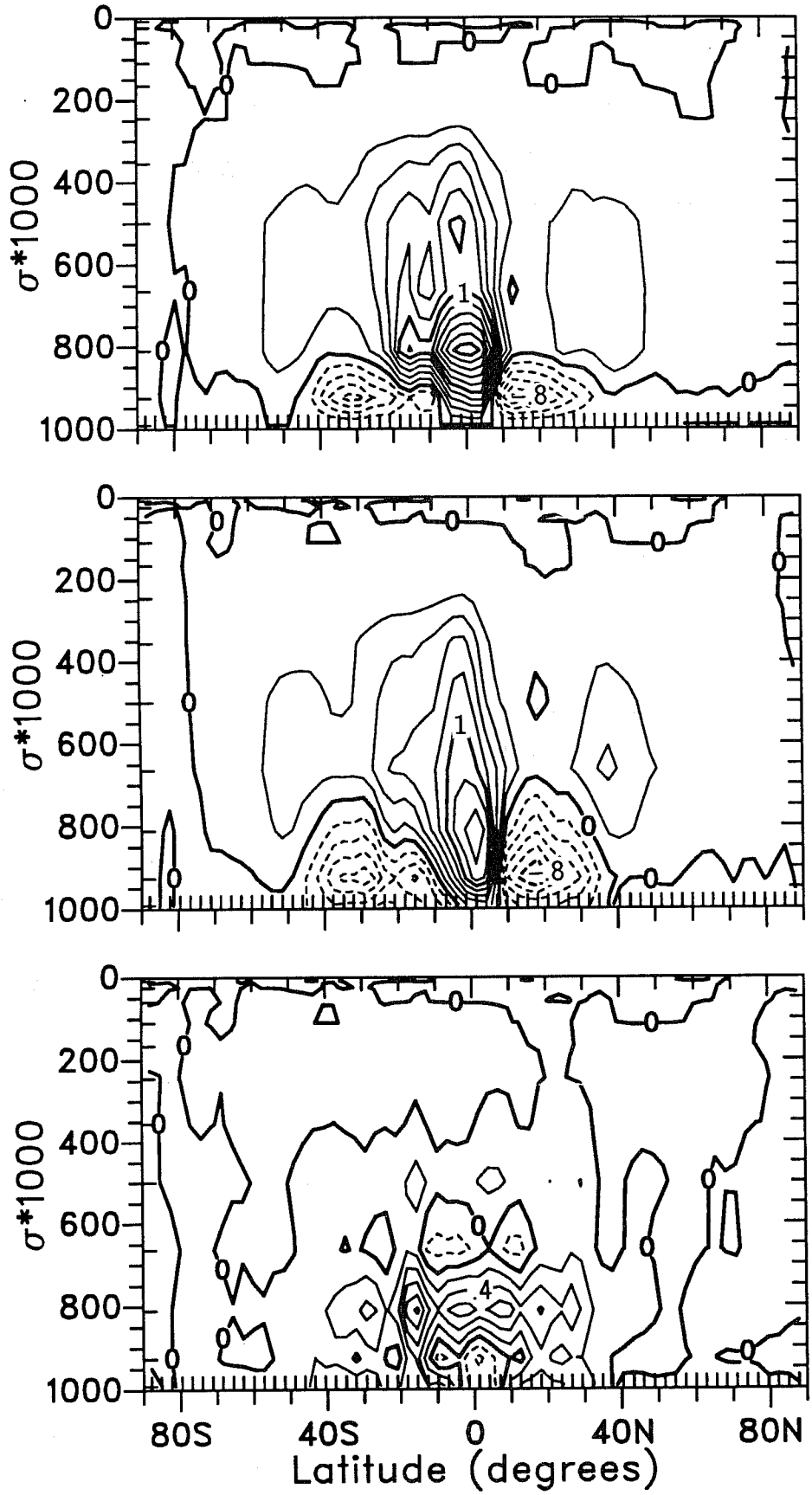

Fig. 9 Time-averaged zonal average of the vertical advection of specific humidity. Top Panel: SLT (contour interval, 0.2 gm Kg^{-1} d^{-1}). *Center Panel:* Spectral (contour interval, 0.2 gm Kg^{-1} d^{-1}). *Bottom Panel:* Differences (contour interval, 0.2 gm Kg^{-1} d^{-1}).

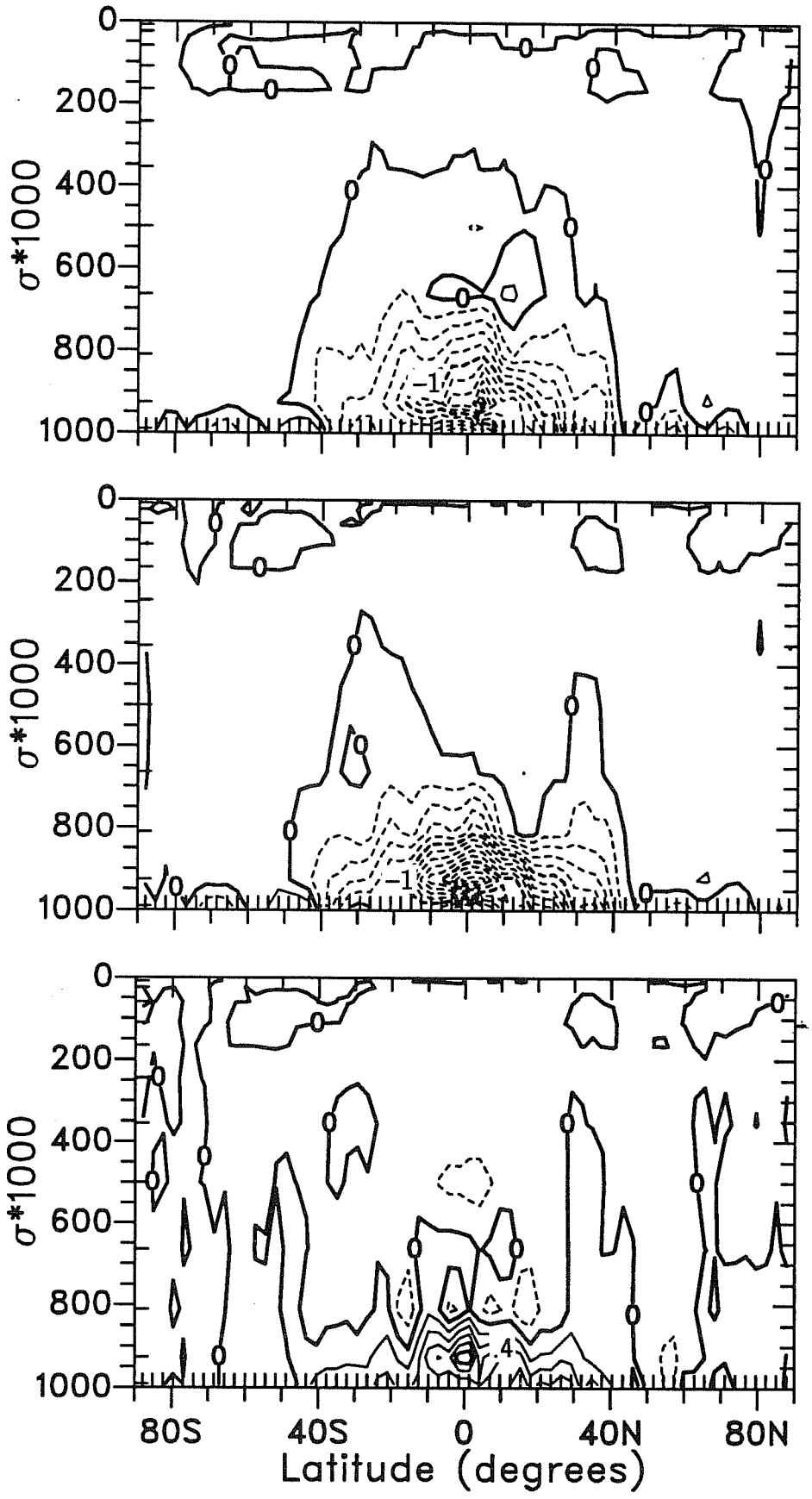

Fig. 10 Time-averaged zonal average of the horizontal advection of specific humidity. *Top Panel:* SLT (contour interval, 0.2 gm Kg^{-1} d^{-1}). *Center Panel:* Spectral (contour interval, 0.2 gm Kg^{-1} d^{-1}). *Bottom Panel:* Differences (contour interval, 0.2 gm Kg^{-1} d^{-1}).

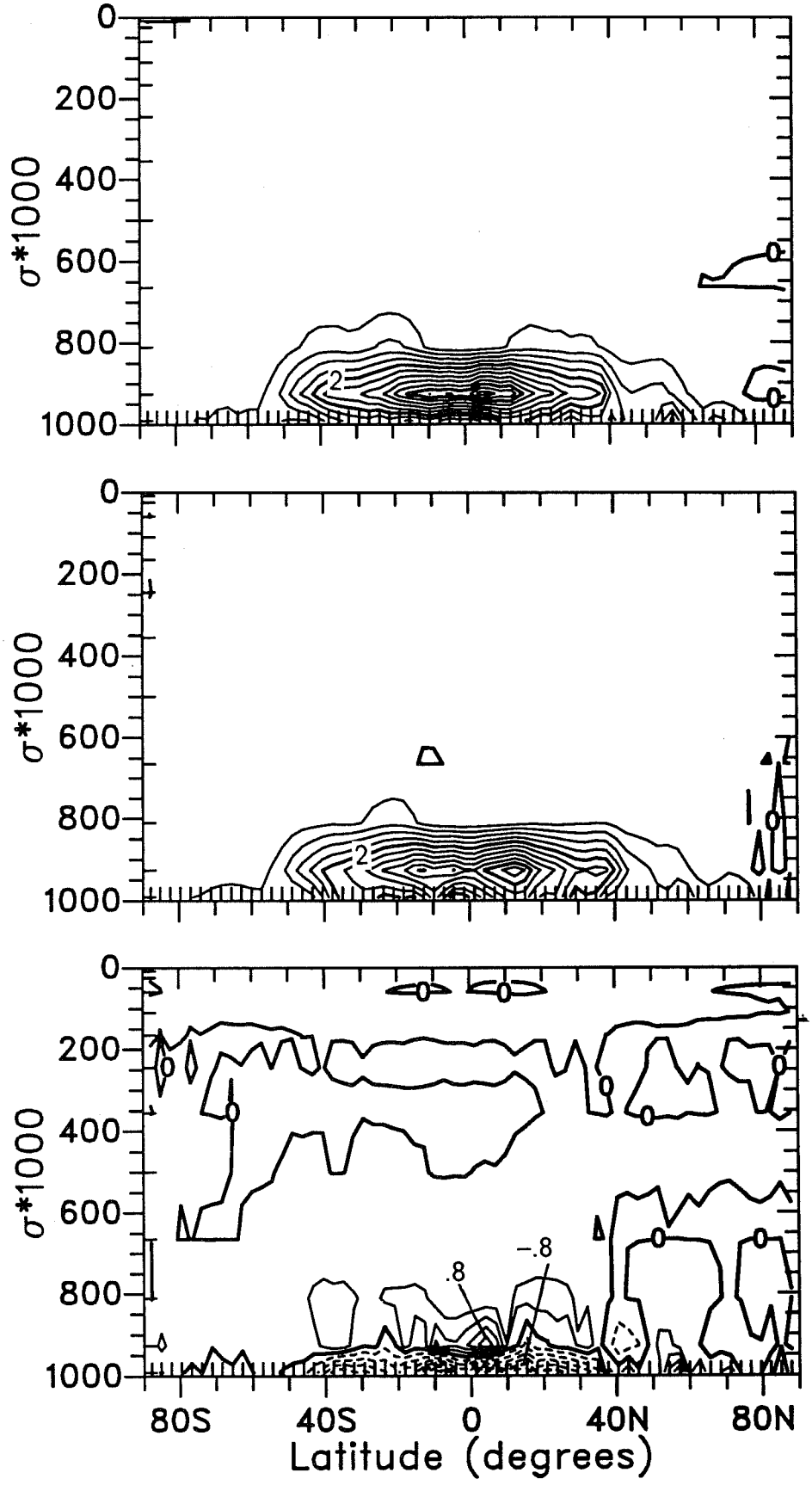

Fig. 11 Time-averaged zonal average of the vertical diffusion and surface flux of specific humidity. *Top Panel:* SLT (contour interval, 0.4 gm Kg^{-1} d^{-1}). *Center Panel:* Spectral (contour interval, 0.4 gm Kg^{-1} d^{-1}). *Bottom Panel:* Differences (contour interval, 0.2 gm Kg^{-1} d^{-1}).

SLT simulated fields produces tendencies which look like the SLT advection of the top panel. Thus the different horizontal advection fields are primarily a result of changes in the balanced states. Note, however that this conclusion is only supported where q is relatively large and well behaved, i.e., equatorward of 60° latitude and below 500 mb. In this situation *Kreiss and Oliger* [1972] have shown that fourth-order methods in some sense are closer to infinite order spectral methods than they are to second-order methods. We will see later that in the polar regions, where the moisture is small the SLT and spectral methods are fundamentally different. In those regions the global least squares minimization of the error implied by the spectral approach is not ideal.

A comparison of the total advection (not shown) suggests that the SLT moistens relative to the spectral in the bottom three model levels (0.811σ and below) equatorward of 50 degrees with a slight drying above. Recall that the specific humidity was larger in the SLT simulation at the third level (0.811σ) but not below (Fig. 1) while the temperature decreased at all levels (Fig. 2). Some process other than advection must be contributing to the drying observed in the SLT simulation in the lowest two levels.

The vertical diffusion and surface fluxes (Fig. 11) are more active in drying the first level and moistening the second in the SLT simulation. Fig. 12 shows that the moist convective adjustment operates to balance the vertical diffusion. Note that the difference in the vertical diffusion is slightly larger than that of the moist convective adjustment, and that both processes are stronger in the second level and weaker in the first in the SLT simulation resulting in the relative vertical gradient in the differences. The net effect of these two processes is to move more water vertically from the first to second model level in the SLT simulation. The vertical diffusion then continues to move the moisture up the the third level in the SLT. The moist adjustment is less active at this level in both models.

This increased vertical flux coupled with the stronger advection in the SLT leads to stronger stable condensation (Fig. 13) in the lower troposphere (below 0.664σ) in the SLT. This increase in stable condensation in the SLT leads to the increased low clouds. In the SLT simulation more points are undergoing stable condensation more often than the spectral control simulation. That is, the same number of points are not simply condensing more moisture when they undergo condensation. The cloud algorithm in CCM1 forms stable clouds with .95 fractional cloudiness in the grid box whenever stable condensation occurs regardless of how much water actually condenses.

The moist adjustment and stable condensation in the upper troposphere in the upward branch of the Hadley cell are stronger in the spectral than the SLT simulation. The stable condensation is also stronger in the spectral simulation in the polar surface areas. These features are discussed more thoroughly in the following paragraphs.

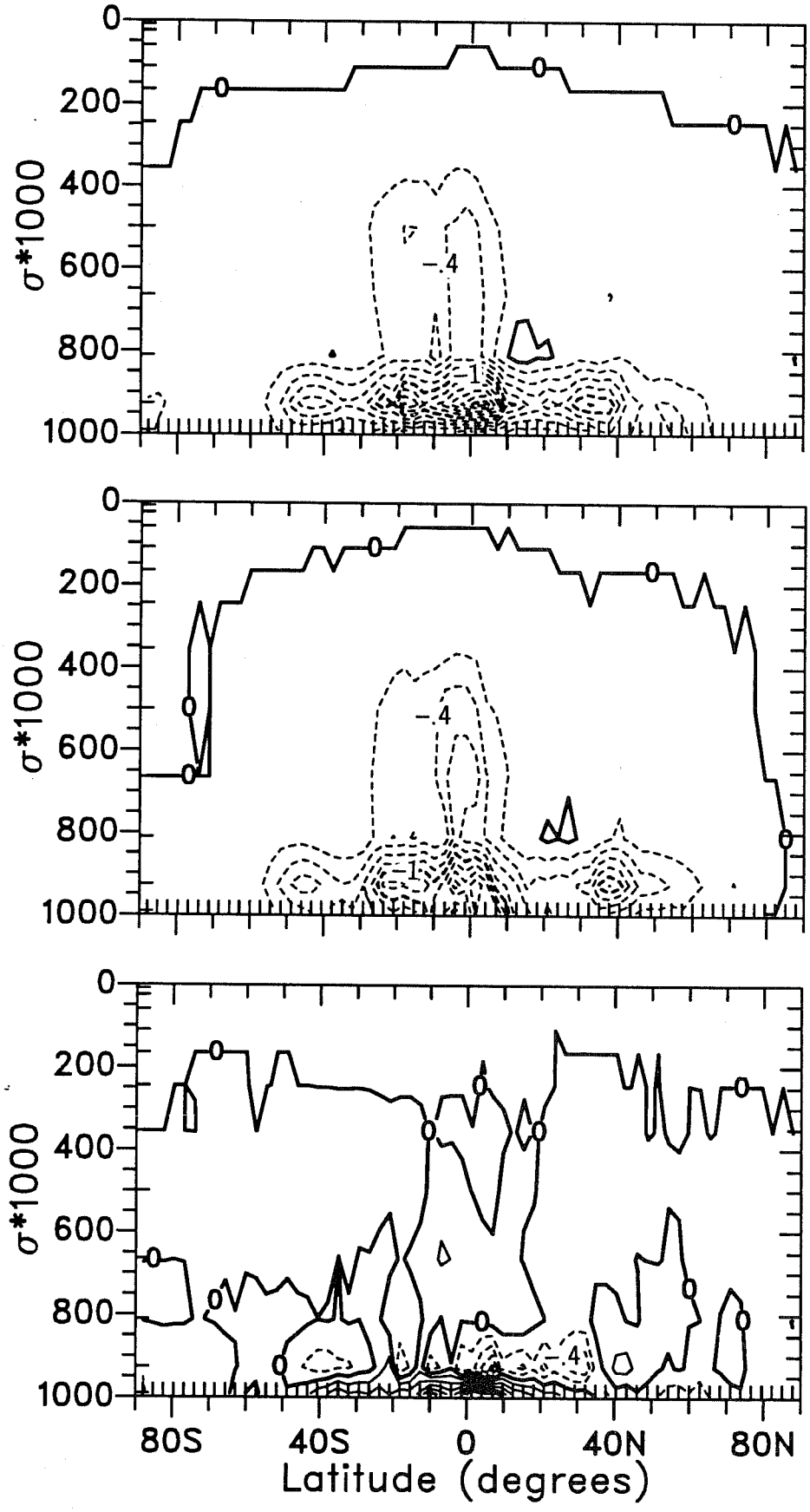

Fig. 12 Time-averaged zonal average of the moist convective adjustment of specific humidity. *Top Panel:* SLT (contour interval, 0.2 gm Kg^{-1} d^{-1}). *Center Panel:* Spectral (contour interval, 0.2 gm Kg^{-1} d^{-1}). *Bottom Panel:* Differences (contour interval, 0.2 gm Kg^{-1} d^{-1}).

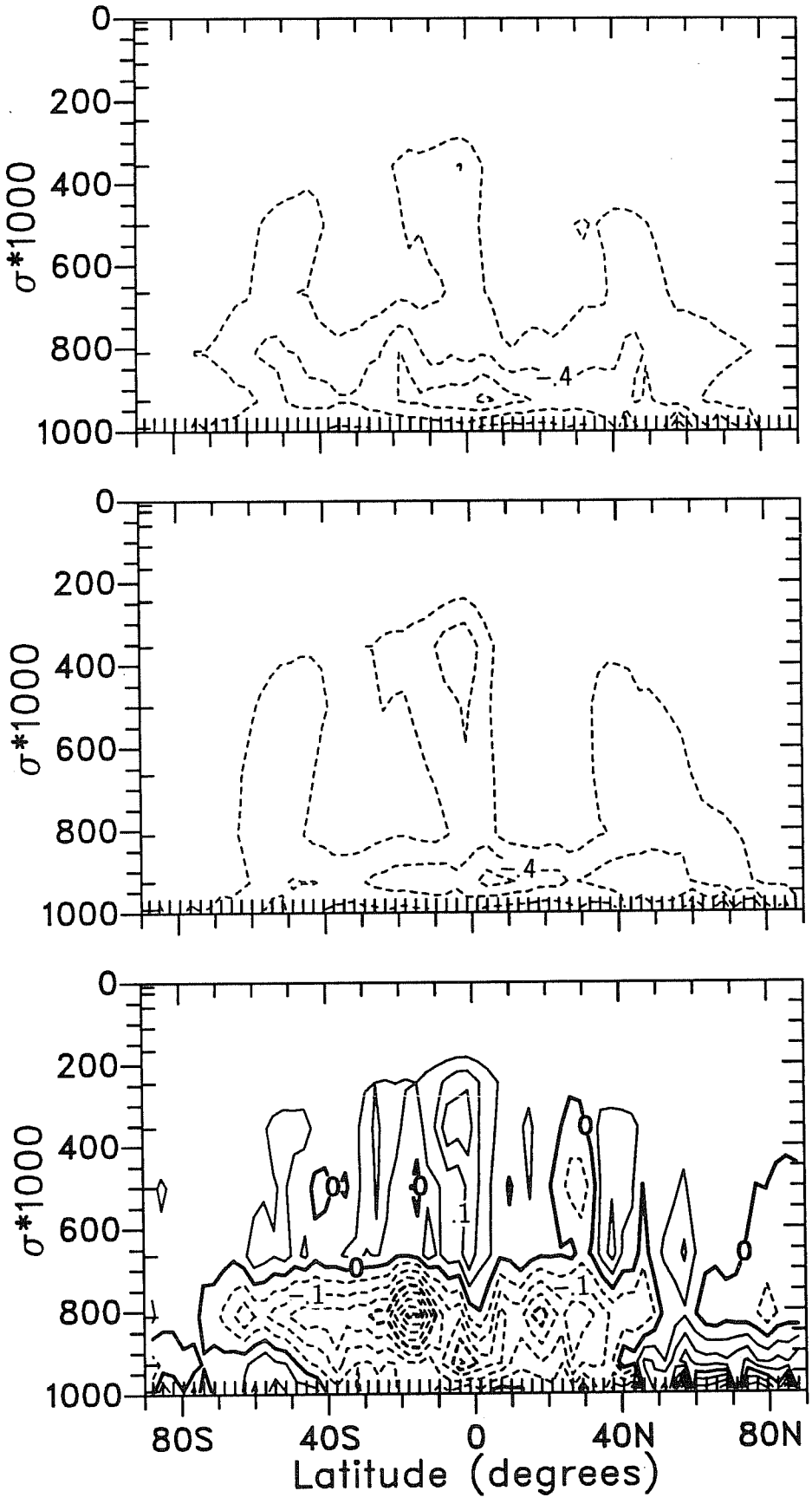

Fig. 13 Time-averaged zonal average of the stable condensation of specific humidity. *Top Panel:* SLT (contour interval, 0.2 gm Kg^{-1} d^{-1}). *Center Panel:* Spectral (contour interval, 0.2 gm Kg^{-1} d^{-1}). *Bottom Panel:* Differences (contour interval, 0.05 gm Kg^{-1} d^{-1}).

Because the specific humidity forecast equation highlights only the lower troposphere away from the polar regions we also examine the various terms after *normalizing* each term by the time mean moisture field. That is, we examine the moisture balance as characterized by inverse time scales. With this normalization (1) becomes

$$0 \approx 1/\tau_{A_h} + 1/\tau_{A_v} + 1/\tau_{D_h} + 1/\tau_{D_v} + 1/\tau_{C_s} + 1/\tau_{C_c} + 1/\tau_F \qquad (2)$$

where, for example

$$1/\tau_{A_h} = \overline{A}_h/\overline{q}$$

is the inverse time scale associated with the horizontal advection of q. This normalization tends to emphasize the importance of the term where it is either very large, or the time-averaged moisture field is small, that is, where the process is changing the field on fast time scales.

The normalized vertical advection corresponding to Fig. 9 appears in Fig. 14. (The difference in the characteristics of the inverse time scales is clear from the plots, and since it is not obvious whether to take the difference before or after normalization, we do not include maps of differences.) The emphasis has changed completely, and the importance of the advective processes near the tropical tropopause becomes apparent. It is clear that the vertical moisture advection is an important mechanism in the upper tropical troposphere in both simulations, and that it plays a more active role in the spectral than in the SLT simulation. In this region the spectral $1/\tau_{A_v}$ is ≈ 3.5 d^{-1} and the SLT $1/\tau_{A_v}$ is ≈ 2.5 d^{-1}. This is so even though the normalizing $\overline{q}$ is somewhat smaller in this region in the SLT simulation. The vertical advection $1/\tau_{A_v}$ peaks one grid level higher in the spectral simulation. The vertical advection is only slightly more active in the spectral simulation in the upper troposphere in the mid-latitude storm track regions. As with the unnormalized vertical advection these differences represent fundamental differences between the numerical methods, and not differences in the state variables. The normalized finite difference vertical advection calculated diagnostically from the SLT simulated states looks like that from the spectral simulation.

The horizontal advection (Fig. 15) is also more active in the spectral simulation in the upper troposphere although it contributes little compared to the vertical advection and the condensation processes considered below. As with the unnormalized horizontal advection below 500 mb, the difference represents a change in the basic state rather than the numerical method. The inverse time scale calculated diagnostically by applying the spectral operators to the SLT simulated state looks like that from the SLT simulation in the vicinity of the tropical tropopause. The spectral advection time scales suggest some moderately fast, rather small scale (in latitude) horizontal advective processes occurring

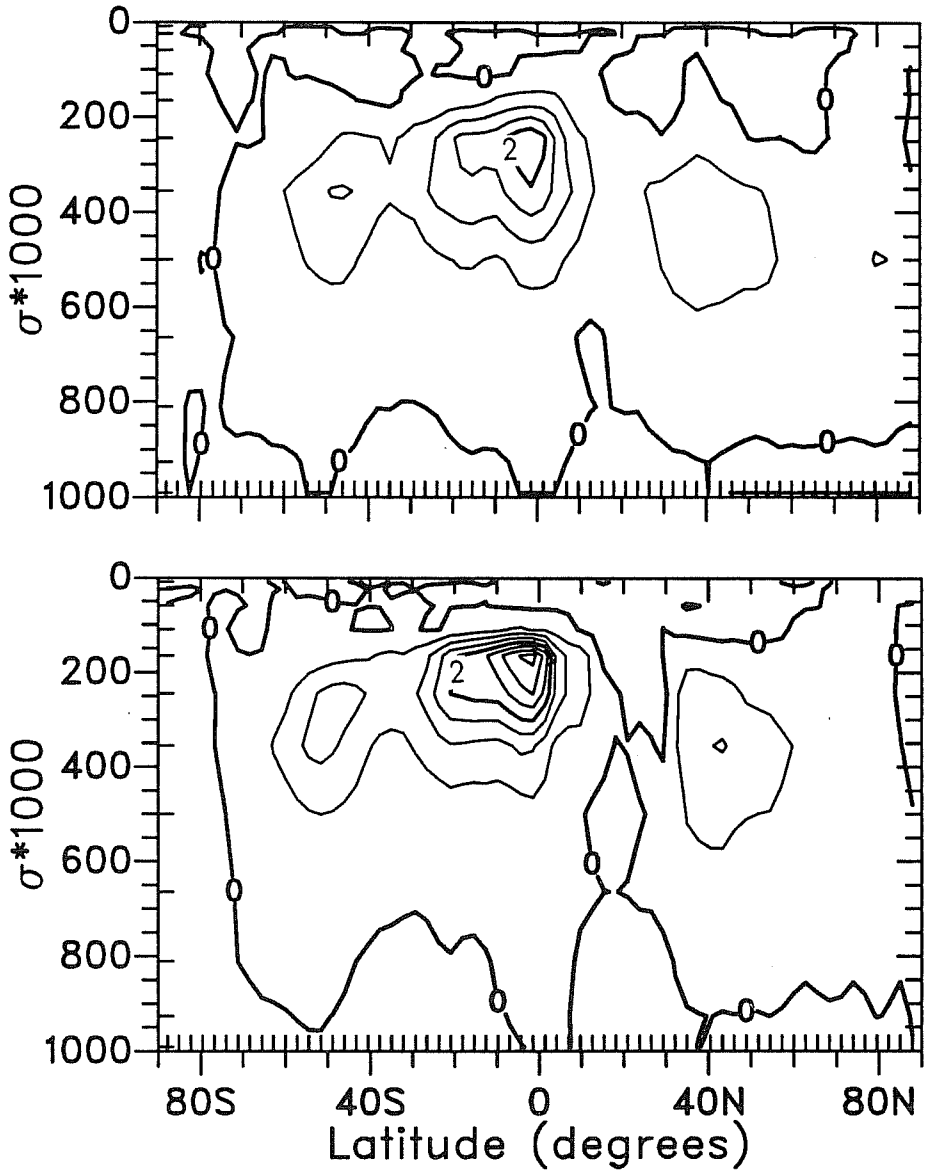

Fig. 14 Time-averaged zonal average of the vertical advection of specific humidity normalized by the time-averaged zonal average specific humidity. *Top Panel:* SLT (contour interval, 0.5 d^{-1}). *Bottom Panel:* Spectral (contour interval, 0.5 d^{-1}).

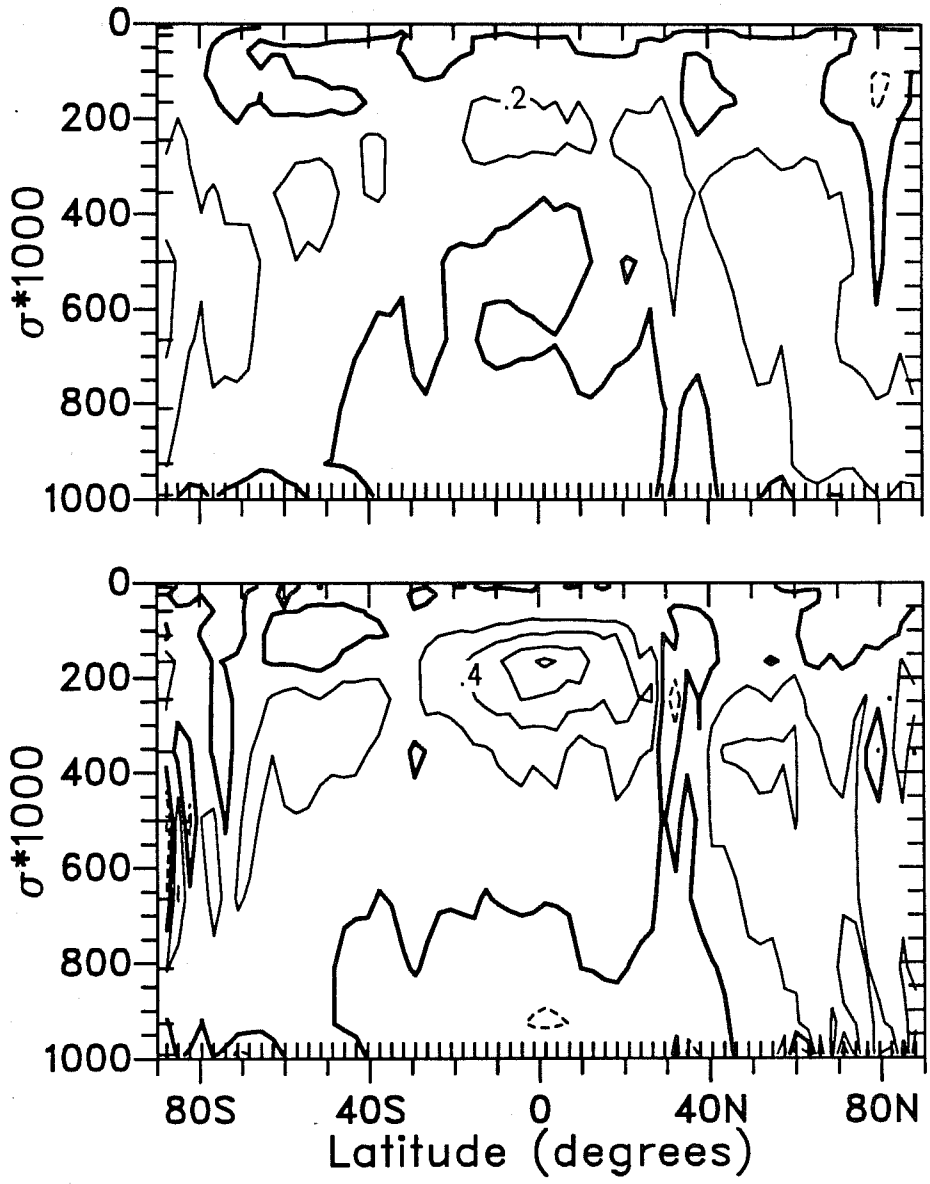

Fig. 15 Time-averaged zonal average of the horizontal advection of specific humidity normalized by the time-averaged zonal average specific humidity. *Top Panel:* SLT (contour interval, 0.2 d^{-1}). *Bottom Panel:* Spectral (contour interval, 0.2 d^{-1}).

in the troposphere in the polar regions and near the surface at the north polar region while the SLT is more coherent in these regions. This difference is associated with the different numerical methods. By definition the horizontal advection includes the spectral truncation inherent in the spectral transform method. In the spectral simulation this seems to be distorting the larger scale advective processes indicated in the SLT simulation. We will return to the implications of this feature after discussing the condensation processes in the upper troposphere.

Fig. 16 shows the inverse time scales for the moist convective adjustment process, which is somewhat more active in the SLT simulation in both the Hadley cell and storm track regions. Fig. 17 shows the inverse time scales for the stable condensation term. The term from the spectral simulation is significantly larger than that from the SLT simulation in these regions (4.5 d^{-1} vs. 1.6 d^{-1}). In fact, in the Hadley cell this term dominates the corresponding advective processes. The vertical diffusion is negligible at these levels and thus is not shown. The extra moisture needed in the spectral simulation to drive the stable condensation at this rate at the tropical tropopause is provided by the negative fixer shown in Fig. 18. The negative fixers are replenishing moisture with a timescale of almost one day in the spectral simulation. This is faster than either the horizontal advection or moist convective adjustment there. (Note that the contour interval for the SLT conservative fixer is 100 times smaller than that for the negative fixer of the spectral simulation.)

The stable condensation is most active one model level higher in the spectral than SLT simulation. This shift along with the slower time scale accounts for the decrease in high clouds seen in the SLT compared to the spectral simulation (Fig. 3).

As mentioned earlier the horizontal advection of the spectral simulation (Fig. 15) exhibits a rather noisy structure in the mid-tropospheric polar regions and near the surface in the north polar region. This is indicative of the problem with the spectral method which requires the inclusion of the negative fixers. Fig. 18 shows that these computational fixer terms become very important in these regions. They are required because of the spectral advection but are ultimately balanced by the stable condensation (Fig. 17). The stable condensation is responsible for the increased cloud (negative area in the difference panel) seen above 500 mb in the spectral simulation at the South Pole. The stable condensation at the surface in the north polar region does not affect the cloud cover as clouds are not formed in the first model level in the model. If they were allowed to form there they would undoubtedly have a significant impact on the simulation. Note that the computational fixer is negligible in the SLT simulation, and no response to it can be identified in any of the physical processes.

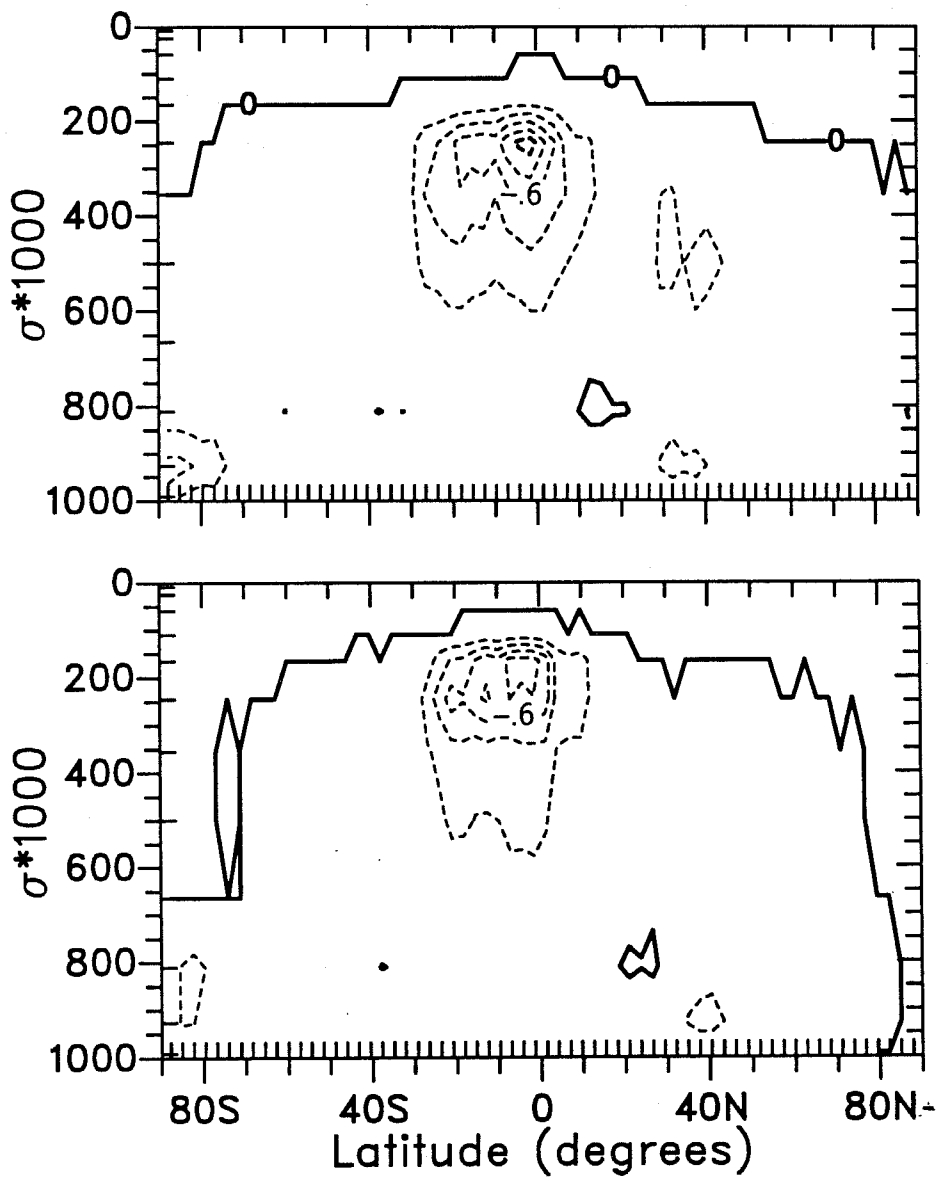

Fig. 16 Time-averaged zonal average of the moist convective adjustment of specific humidity normalized by the time-averaged zonal average specific humidity. *Top Panel:* SLT (contour interval, 0.2 d^{-1}). *Bottom Panel:* Spectral (contour interval, 0.2 d^{-1}).

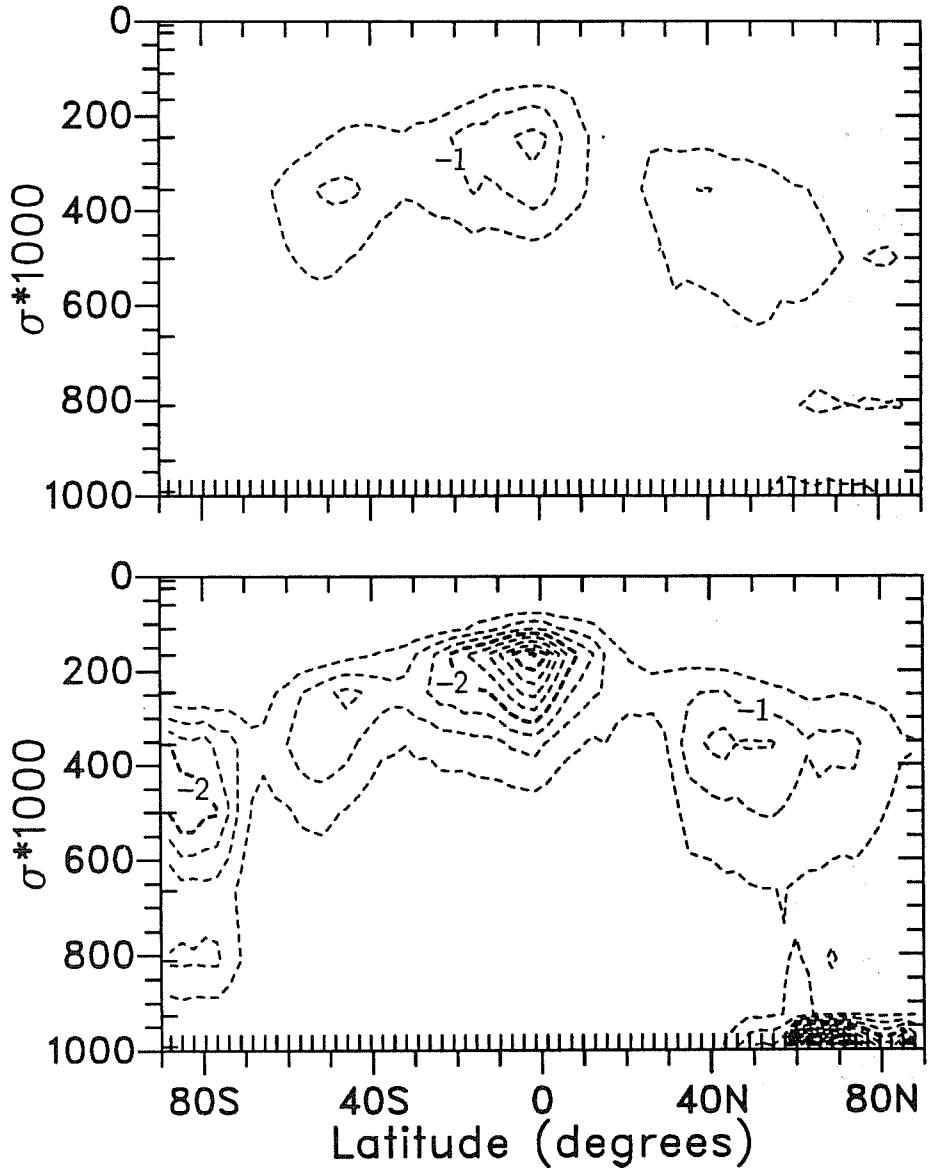

Fig. 17 Time-averaged zonal average of the stable condensation of specific humidity normalized by the time-averaged zonal average specific humidity. *Top Panel:* SLT (contour interval, 0.5 d^{-1}). *Bottom Panel:* Spectral (contour interval, 0.5 d^{-1}).

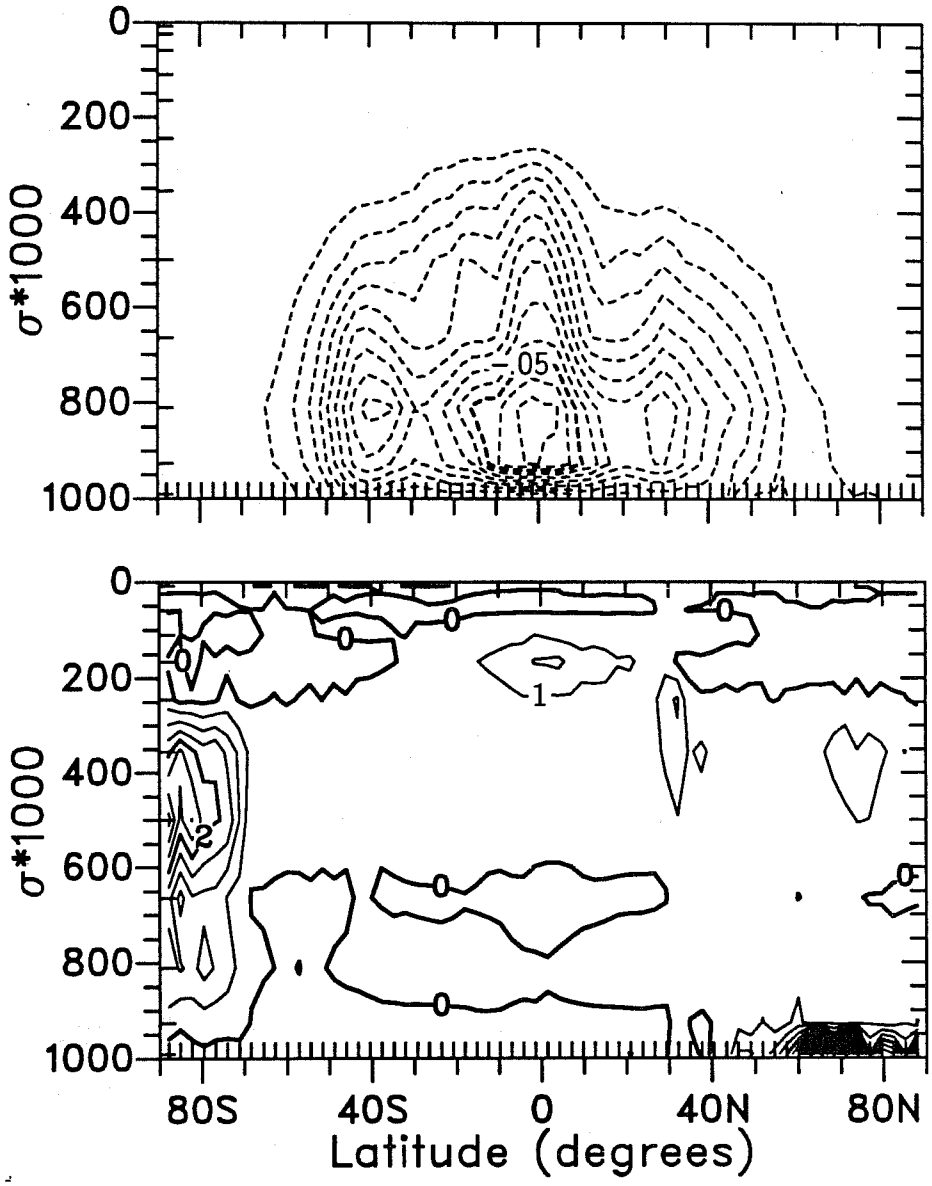

Fig. 18 Time-averaged zonal average of the specific humidity fixers normalized by the time-averaged zonal average specific humidity. Note the different contour intervals. *Top Panel:* Conservation adjustment in SLT (contour interval, 0.005 d^{-1}). *Bottom Panel:* Negative fixers in spectral (contour interval, 0.5 d^{-1}).

5. REMARKS AND CONCLUSIONS

The climate simulated by the spectral CCM1 at T42 horizontal resolution has been compared to one with the spectral transport of water vapor replaced with a shape preserving semi-Lagrangian scheme (SLT). The model climate is strongly dependent on the water vapor transport scheme. The model troposphere is everywhere colder in the SLT simulation except in the polar surface areas which are warmer. The stratosphere is warmer in the SLT simulation. The SLT simulation is drier above 800 mb and in the lowest model levels and moister around 800 mb. More importantly the SLT simulation has significantly more low clouds and a slight decrease in high clouds around the tropical tropopause.

Obviously the ultimate cause of the different simulations is the different water vapor advection algorithm as that is the only component changed. This advection affects the simulation directly by changing the water vapor distribution and release of latent heat, and indirectly by modulating the radiative heating. The change in water vapor distribution results in radiative changes via the absorption by the water vapor itself and through changes in the cloud properties and distribution.

Some of the differences in the simulations are directly attributable to the advection algorithms themselves. Calculation of the advective tendencies with the two advection schemes (using the same specified moisture and velocity fields) can result in quite different estimates of the tendencies. Other of the differences in the simulations are due to the negative fixer. These differences in turn effect the physical processes and via complicated feedbacks mechanisms a new climate equilibrium is achieved. We summarize and synthesize the results of this study in the following paragraphs.

The two vertical advection schemes are fundamentally different and provide a primary difference in the forcing. The vertical finite difference scheme used in the spectral model for vertical advection has only a formal first-order accuracy for unevenly distributed sigma layers. The vertical advection proceedure in the SLT scheme is formally fourth-order accurate for smooth fields even for unequal sigma level distributions. When the vertical advection by finite differences is used in a diagnostic sense on the fields simulated by the SLT model the vertical moisture advection tendencies resemble those of the spectral model simulation rather those of an SLT model simulation. From this we conclude that the different vertical advection process observed in the two simulations is not a secondary response to changes in the atmospheric state but is a first-order response to differences in the numerical algorithm. Such a different behavior is not surprising since the two schemes have different formal accuracy and the vertical grid is very coarse, especially when dealing with a field such as water vapor which changes by several orders of magnitude in the domain. The averaging inherent in the vertical finite difference approximation

tends to smooth the term across grid levels while the semi-Lagrangian scheme is capable of maintaining more structure as seen in Fig. 9. This is also seen at the lowest model level which feels the surface boundary condition (that the vertical velocity be zero) more strongly in the SLT approximation. With increased vertical resolution the finite difference approximations behave more like the SLT at the first model level.

The differences in the horizontal transport are somewhat more difficult to sort out. The formal accuracy of both schemes is high and statements relating formal accuracy to the character of the simulations are difficult. Where the mixing ratio is relatively large, i.e. below 500 mb and equatorward of 60 degrees latitude, the signal seen in the horizontal advection reflects the changed simulated state and does not represent a primary difference between the two approaches. The spectral approximations applied diagnostically to the fields simulated by the SLT scheme result in an advection pattern that looks like that of the SLT simulation. This similarity also holds above 500 mb in the tropics when diagnosed via the inverse time scale. However, in the polar regions where the mixing ratio is relatively small the inverse time scales show that the spectral and SLT approximations behave very differently. The spectral approach shows fast processes switching between signs on a relatively small latitudinal scale while the SLT exhibits rather coherent structures with slower time scales. This behavior is also observed in the implied inverse time scale if the spectral approximation is applied diagnostically to the SLT simulated states. The noise in the spectral approach is presumably caused by the spectral truncation and the global aspects of the spectral transport algorithm which are integral components of the method.

The sum of the vertical and horizontal advection tends to moisten the lower troposphere equatorward of 50 degrees latitude in the SLT simulation relative to the spectral and dry the upper tropical troposphere. This different behavior leads to changes in other processes, particularly condensation and its associated cloud formation, which have strong affects on the model climate.

In the polar regions the negative advective tendencies of the spectral method are large enough to produce negative specific humidity values. The negative fixer included in the spectral model operates as a compensating moisture source in those regions. Although the fixer only brings the moisture up to zero at the negative points, it increases the overall moisture in these regions and its net effect has a strong influence on the precipitation and clouds there. This is particularly noticeable in the summer pole mid-tropospheric levels and winter pole surface level stable condensation. In the upper tropical troposphere the negative fixer also contributes to the moisture available for stable condensation. The contribution of the fixer to the climate balance of the spectral model in the upper tropical troposphere and winter polar surface regions does not decrease with increased horizontal

resolution [*Kiehl and Williamson*, 1991] at least up to T106 resolution. The variational adjustment included in the SLT version to maintain conservation of moisture in the advective step shows no sign of interacting with any of the physical processes examined here. It does not seem to influence the model climate.

The model climates from the two different systems involve delicate balances between the various components of the atmospheric system. In studying the climates produced by such balances it is difficult to isolate cause and effect. Nevertheless some features stand out from our study. In mid-latitudes and tropics, low clouds increase due to stronger advection and stronger vertical diffusion which lead to stronger stable condensation in the SLT simulation. The stronger vertical diffusion is related to different vertical gradients of moisture and temperature. The spectral simulation has more tropical high clouds in part due to stronger vertical advection and in part due to the fixer there. The spectral simulation has more mid level clouds in the south polar region due to the negative fixer. The fixer is also very active at north polar surface region where it is balanced by stable condensation. This is not seen in the cloud field as clouds are not allowed to form in the surface layer but does lead to a heat source as discussed in section 4.2.

Slingo [1990] has suggested that for reasonable confidence in understanding the influence of low clouds on climate, a minimum relative accuracy of 5% in modeling their radiative effect is required, with even more stringent requirements for their component radiative properties (cloud fraction, liquid water path, and mean droplet radius). This study suggests that even if the physical foundations of the parameterization were understood perfectly, errors in the numerical algorithms associated with moisture transport can influence the cloud amount and distribution by much more than that. Errors in the spectral method and the fixers required to partially compensate them clearly have a large effect on the moisture budget and thus on the model climate. Other errors are more difficult to identify directly from climate simulations. However, the differences in the characteristics of the two schemes used here, for example the vertical advection, indicate that numerical algorithms may not safely be ignored, and one cannot focus only on the physical parameterizations. It is clear that both the physical parameterizations, and the numerical techniques used to approximate the atmosphere are having an affect on the simulation.

The semi-Lagrangian scheme addresses the problems noted with the spectral method. We should not regard the colder and drier simulated atmosphere of the semi-Lagrangian version as implying a poorer representation of the water vapor transport process. The CCM1 is a model which has been (perhaps inadvertantly) tuned with respect to spectral moisture transport. Changing only one component as done here without retuning the others can eliminate a fortuitous balance of errors. In addition CCM1 is missing some

important components such as a shallow convection parameterization which can have a very significant impact on the model climate. We have not attempted to retune CCM1 with semi-Lagrangian moisture transport. This exercise has been performed with the next version of the CCM (CCM2) which includes the semi-Lagrangian transport of moisture and trace species as well as all physical process parameterizations modified or replaced.

Although the sensitivity of a GCM to moist processes like shallow non-precipitating convection or the assumptions within a deep convective parameterization is well known, we have found this sensitivity to have increased in the presence of the SLT scheme. For example, we have found that the change in climate associated with replacing the (currently standard) moist convective adjustment scheme with a Kuo style penetrative convective scheme is quite different depending on the moisture transport scheme. The depth of heating associated with the change increases more when the SLT is in place. In addition, gridpoint storms are much reduced, and the atmospheric moistening and warming is increased when SLT is used compared to when spectral transport is used. We offer this anecdote to reaffirm our conviction that the numerical methods used in climate models continue to require attention and should not be neglected in our ongoing attempts to understand the physics of the atmosphere.

It has occasionally been proposed to us that that the sensitivity of a GCM to the transport scheme would be less for a model with more sophisticated physics, and presumably more realistic moisture structures. For this to be true, one must presuppose that either: 1) the advection terms are playing too important a role in the CCM simulation and that some process either missing or poorly handled in the CCM ought to be controlling the moisture distribution; or 2) that the physical processes which are in the CCM are overly sensitive to the distribution of water vapor. We believe that the second item is quite unlikely. All improvements to the physical parameterizations that we can anticipate, or have experimented with to date, lead to more, rather than less sensitivity to the moisture distribution. We do acknowledge that this version of the CCM has a very simple representation of the physical processes regulating moisture in the lower troposphere and tropics. Any process which acts to "mix" the atmosphere more thoroughly and thus reduce the gradients of water vapor ought to reduce the sensitivity to the transport formulation. It is clear that parameterizations for processes like shallow convection would more actively vent the boundary layer and result in an overall moister atmosphere. A more realistic deep convection scheme could result in increased transport of water vapor to the upper tropical troposphere. While this may reduce the mean vertical gradient of moisture through the depth of the troposphere it could also increase local gradients and the troposphere/stratosphere gradient and thus increase the need for an accurate vertical transport algorithm. On the other hand we have shown that many of the problems we have

found occur in regions where few other processes occur (e.g. the polar regions). Unless some process acts to "mix" the atmosphere more thoroughly and thus reduce the gradients of water vapor, one need not expect any reduction of the problems with the borrower in the vicinity of the pole. It is impossible to anticipate the results of a sensitivity study in a more sophisticated model. We will however have such a model at our disposal (the NCAR CCM2) and will perform such a study in the future.

Acknowledgements

Thanks to Brian Eaton and Jerry Olson for their assistance in developing the required computer code. We thank B. Briegleb for providing the ERBE data in an easy to process form. We also acknowledge the assistance of Eileen Boettner in the final preparation of the manuscript. We benefited greatly from many discussion with colleagues and visitors to our section. Our conversations with J. T. Kiehl were particularly invaluable. We would also like to thank J. J. Hack for his comments on an earlier draft. A portion of this research was funded through U.S. Navy contract N6668568WR86062.

References

Brackbill, J. U. and L. G. Margolin, An algorithm for the computation of nonlinear electron thermal conduction on an arbitrarily shaped, two-dimensional domain, Los Alamos Scientific Laboratory, *LA-6964-MS*, Los Alamos, N. M., 47 pp., 1977.

Hack, J. J., L. M. Bath, G. S. Williamson and B. A. Boville, Modifications and enhancements to the NCAR Community Climate Model (CCM1), National Center for Atmospheric Research, *NCAR Tech. Note, NCAR/TN-336+STR*, Boulder, Colo., 97 pp., 1989, Gov't ordering no. NTIS PB89–215594/AS.

Isaacson, E., Integration schemes for long-term calculation, in *Second IMACS (IACA) Meeting on Advances in Computer Methods for Partial Differential Equations*, edited by R. Vichnevetsky., International Symposium on Computer Methods for Partial Differential Equations, pp. 251–255, IACA, Lehigh University, Bethlehem, Pa., 1977.

Kiehl, J. T. and V. Ramanathan, Comparison of cloud forcing derived from the Earth Radiation Budget Experiment with that simulated by the NCAR Community Climate Model, *J. Geophys. Res.*, *95*, 11,679–11,698, 1990.

Kiehl, J. T. and D. L. Williamson, Dependence of cloud amount on horizontal resolution in the NCAR Community Climate Model, *J. Geophys. Res.*, 1991, in press.

Kreiss, H. -O. and J. Oliger, Comparison of accurate methods for the integration of hyperbolic equations, *Tellus*, *24*, 199–215, 1972.

Manabe, S., J. Smagorinsky and R. F. Strickler, Simulated climatology of a general circulation model with a hydrologic cycle, *Mon. Weather Rev.*, *93*, 769–798, 1965.

McFarlane, N. A., The effect of orographically excited gravity wave drag on the general circulation of the lower stratosphere and troposphere, *J. Atmos. Sci.*, *44*, 1775–1800, 1987.

Peixoto, J. P. and A. H. Oort, The atmospheric branch of the hydrological cycle and climate, in *Variations in the Global Water Budget*, pp. 5–65, D. Reidel, Hingham, Mass., 1983.

Ramanathan, V., The role of earth radiation budget studies in climate and general circulation research, *J. Geophys. Res.*, *92*, 4075–4095, 1987.

Ramanathan, V., R. D. Cess, E. F. Harrison, P. Minnis, B. R. Barkstrom, E. Ahmad and D. Hartmann, Cloud-radiative forcing and climate: Results from the Earth Radiation Budget Experiment, *Science*, *243*, 57–63, 1989.

Ramanathan, V., E. J. Pitcher, R. C. Malone and M. L. Blackmon, The response of a spectral general circulation model to improvements in radiative processes, *J. Atmos. Sci.*, *40*, 605–630, 1983.

Rasch, P. J. and D. L. Williamson, On shape-preserving interpolation and semi-Lagrangian transport, *SIAM J. Sci. Stat. Comput.*, *11* , 656–687, 1990a.

Rasch, P. J. and D. L. Williamson, Computational aspects of moisture transport in global models of the atmosphere, *Q. J. R. Meteorol. Soc.*, *116*, 1,071–1,090, 1990b.

Ritchie, H., Application of a semi-Lagrangian integration scheme to the moisture equation in a regional forecast model, *Mon. Weather Rev.*, *113*, 424–435, 1985.

Sasaki, Y. K., Variational design of finite-difference schemes for initial value problems with an integral invariant, *J. Comput. Phys.*, *21*, 270–278, 1976.

Slingo, A., Sensitivity of the Earth's radiation budget to changes in low clouds, *Nature*, *343*, 49–51, 1990.

Slingo, A. and J. M. Slingo, The response of a general circulation model to cloud longwave radiative forcing. I: Introduction and initial experiments, *Q. J. R. Meteorol. Soc.*, *114*, 1027–1062, 1988.

Takacs, L. L., Effects of using a posteriori methods for the conservation of integral invariants, *Mon. Weather Rev.*, *116*, 525–545, 1988.

Trenberth, K. E., J. R. Christy and J. G. Olson, Global atmospheric mass, surface pressure and water vapor variations, *J. Geophys. Res.*, *92*, 14,815–14,826, 1987.

Williamson, D. L., Semi-Lagrangian moisture transport in the NMC spectral model, *Tellus*, *42A*, 413–428, 1990.

Williamson, D. L., J. T. Kiehl, V. Ramanathan, R. E. Dickinson and J. J. Hack, Description of NCAR Community Climate Model (CCM1), National Center for Atmospheric Research, *NCAR Tech. Note, NCAR/TN-285+STR*, Boulder, Colo., 112 pp., 1987, Gov't ordering no. NTIS PB87–203782/AS.

Williamson, D. L. and P. J. Rasch, Two-dimensional semi-Lagrangian transport with shape preserving interpolation, *Mon. Weather Rev.*, *117*, 102–129, 1989.